Effects of Common E-Cigarette Compounds on Immortalized Mouse Hepatocytes and Glutathione as a Potential Modulator of Susceptibility

Michael Anderson

A thesis

submitted in partial fulfillment of the

requirements for the degree of

Master of Science

University of Washington

2020

Committee:

Terrance Kavanagh (chair)

Elaine Faustman

Edward Kelly

Program Authorized to Offer Degree:

Department of Environmental and Occupational Health Sciences

University of Washington

Abstract

Effects of Common E-Cigarette Compounds on In-Vitro Cell Viability and Glutathione as a Potential Modulator of Susceptibility

Michael Anderson

Chair of the Supervisory Committee:

Terrance Kavanagh

Department of Environmental and Occupational Health Sciences

In 2018, 3.2% of adults reported currently using an e-cigarette (vaping) at least once in a 30-day period[1]. 20.8% and 4.9% of high school and middle school students, respectively, also reported using e-cigarettes during that same year[2]. Of greater concern, in 2019, 27.5% of high school students and 10.5% of middle school students reported using e-cigarettes[3]. Despite this, comparatively little research has been done on the potential hazards and effects of e-cigarettes. In this study, four compounds were chosen due to their common associations with various aspects of vaping. Formaldehyde and acetaldehyde were chosen as common pyrolysis byproducts of the propylene glycol/vegetable glycerin vehicle found in most vaping formulations; cinnamaldehyde and diacetyl were chosen as common flavoring agents. Immortalized mouse hepatocytes were used as a model system for this study with the hope that this would limit any confounding

associated with approaching senescence. Two cell lines—either sufficient or deficient in the production of the antioxidant glutathione (GSH) (*Gclm* wild-type of null cells, respectively) were exposed to each of the four compounds in culture. Effects on viability, antioxidant response, oxidative stress, and gene expression were then evaluated. Formaldehyde and cinnamaldehyde showed the most profound effects on overall viability, while acetaldehyde showed virtually no effect. Diacetyl only demonstrated nominal effects up to the highest dose. Similarly, formaldehyde and cinnamaldehyde showed drastic decreases in total GSH levels, whereas acetaldehyde and diacetyl showed only modest decreases at low doses that re-approached baseline levels at higher doses. RNAseq revealed differential gene expression in the wild type cells at 100 μM cinnamaldehyde and 1 mM diacetyl; the knockout cells had significant differential gene expression at 250 μM and 1 mM diacetyl. Quantitation of lipid peroxidation levels revealed virtually no significant dose or genotype effects, but even with a lack of significance the *Gclm* null cells appeared to have higher levels of peroxidized lipids across all four compounds. Despite the preliminary nature of the data and the lack of a concrete physiological context, it demonstrates that some of these compounds could potentially pose a hazard to the liver. Further research is needed to better understand the risks posed by these compounds, especially in the context of *in vivo* exposures to e-cigarette aerosols.

Introduction:

Conventional tobacco smoking is a known risk factor for numerous pathologies such as cancer[43] and cardiovascular disease[44]. The risks posed by tobacco smoking are reasonably well understood because decades of research have been dedicated to parsing out underlying mechanisms of effect. Ongoing research continues to reveal any missing links connecting smoking, personal health, and public health. Conversely, the modern-day e-cigarette has only been in existence since the early 2000s, and therefore there has been comparatively little research into the health effects of smoking e-cigarettes (vaping). This is concerning because smoking tobacco and vaping are not the same, meaning that any of the issues and health effects associated with smoking tobacco may not be applicable to vaping. Smoking involves the combustion of tobacco and potential additives such as menthol, humectants, sugars, and ammonium compounds—resulting in over 4700 potential end products.[35,36] Since tobacco is the main component of conventional cigarettes, these additives tend to comprise only 1-5% of the total constituents. [35] Vaping involves the heating, pyrolysis, and subsequent aerosolization of various chemical components: humectants, nicotine, flavoring agents, and more recently cannabinoids[1]. This results in some of these additives becoming more primary components in vaping liquids. Each of these components brings a unique dimension to assessing the potential hazards and risks, and the relative composition of each liquid formulation introduces even more variability. Additionally, some models of e-cigarette allow the heating temperature to be adjusted[1] which may chemically alter some of the base constituents, adding yet another new dimension to the problem. Characterizing the different end products of vaping is an ongoing topic of research.

Statistics show that as of 2018, 3.2% of adults in the United States reported recently (within the last 30 days) using e-cigarettes.[2] During that same year, 20.8% and 4.9% of high

school and middle school students respectively reported currently using e-cigarettes.[3] Even more concerning is the fact that in 2019, 27.5% of high school students and 10.5% of middle school students reported using e-cigarettes.[4] The prevalence in both populations outstrips conventional tobacco smoking by a factor of five.[4] Clearly, vaping is an issue disproportionately affecting youth. Potential reasons for this include use by friends or family, the variety of flavors available, and the perceived safety of the products relative to conventional tobacco cigarettes.[5]

This last reason is especially poignant given the recent outbreak of e-cigarette or vaping associated lung injury (EVALI) in 2019. In total, 2807 hospitalizations and 68 deaths were reported to the CDC.[6] The condition was linked to the presence of vitamin E acetate, primarily in THC containing formulations of vaping liquid. The compound is "generally regarded as safe" (GRAS), and can commonly be found in dietary supplements and cosmetics. However, the GRAS status only applies to oral and dermal exposures, whereas vaping presents these compounds via a respiratory exposure; in fact, a recent study by Wu and O'Shea posited that vitamin E acetate may be chemically changed to the toxic gas ketene when exposed to vaping relevant temperatures—a breakdown pathway that would likely never need to be considered when dealing with its other uses.[37] The perception of safety is likely born from a lack of knowledge about how these compounds affect the body with this novel exposure pathway. However, as more research has been undertaken there has been an increasingly defined connection between vaping and various adverse health outcomes.

When looking at the process as a whole, vaping has been implicated in a host of adverse effects ranging from inflammation to reactive oxygen species generation across multiple different body systems.[7,8,9] This is unsurprising given the complex chemical mixtures found in vaping liquids, with many components consisting of reactive carbonyls. This also makes

assessing health effects harder because the liquids are mixtures. Some of the current research—this study included—is approaching the issue on a per-compound basis.

This study seeks to identify possible adverse effects associated with exposure to formaldehyde, acetaldehyde, cinnamaldehyde, and diacetyl. The first two compounds are common byproducts of the pyrolysis of the propylene glycol/vegetable glycerin vehicle found in many formulations of vaping liquids. The latter two compounds are common flavoring agents. Since these compounds are all reactive carbonyls, the underlying hypothesis is that the ubiquitous antioxidant glutathione (GSH) will be protective when dealing with exposures from these chemicals.

GSH is well known for playing an active role in detoxifying harmful compounds and metabolites. A classic example is that of acetaminophen (APAP) metabolism and elimination. If the body's sulfation and glucuronidation phase-II pathways are overwhelmed (as can occur with APAP overdose), GSH can be conjugated to APAP's toxic metabolite n-acetyl-p-benzoquinoneimine (NAPQI) by glutathione-S-transferases (GSTs) to prevent organ damage.[20,21] Additionally, GSH is also critical in detoxifying hydroxyl radicals and other reactive oxygen species that are detrimental to overall cell health. These processes are dependent on the efficient production of GSH, which is largely governed by the expression of the glutamate cysteine ligase catalytic and modifying subunits (*Gclc* and *Gclm* respectively). Under most circumstances GCL activity is rate-limiting for GSH synthesis.[47] This project makes use of two immortalized mouse hepatocyte cell lines to probe how GSH modulates the effects of exposure to the four previously stated vaping chemicals. One line is sufficient in *Gclm* (wild type) while the other has had the *Gclm* gene disrupted ("knocked out"; *Gclm* null), which serves to represent individuals with chronically low GSH production. Both cell lines were taken from the livers of mice with the

corresponding genotype. This model has been used in past experiments in an *in vivo* setting. Results from those experiments have demonstrated that the *Gclm* knockout genotype tends to exhibit greater sensitivity to oxidative stress and toxic insults across multiple organ systems.[22,23,24] The specific model used by this lab has been characterized by McConnachie et al.[22] One study demonstrates that *Gclm* null fibroblasts have been shown to enter a senescent state earlier than wild type fibroblasts with accompanying changes in population doubling time, morphology, and gene expression.[34] Therefore, by immortalizing the hepatocytes from these model animals, we are ideally able to reduce any potential variability associated with approaching senescence while in culture.

To date, this is one of the few studies to look at potential vaping impacts on the liver.[25,38,48,49] While not experiencing the amount of exposure the lungs do, the liver can act as the second line of defense for any vaped material that enters systemic circulation. Given the relatively easier absorption across alveolar membranes when compared to other barriers, the level of vaped material crossing from the lungs into the blood is likely not insignificant. Therefore, the liver will be important for detoxifying any compounds that do cross into the blood.

Methods:

Cell culture

The immortalized *Gclm* wild type and knockout mouse lines were generated by crossing transgenic mice expressing a temperature-sensitive, interferon-γ induced large T-antigen with *Gclm* heterozygote mice; subsequent inter-crosses resulted in *Gclm* wild type, heterozygote, and knockout “immortamice”. Cells were isolated from livers with the appropriate genotype and

expanded in culture. Only *Gclm* wild type and knockout hepatocyte lines were used for this project, and they were maintained on supplemented Williams-E medium (Life Technologies, Grand Island, NY). To each 500 mL bottle of medium the following were added: 5 mL of 1 M nicotinamide, 5 mL of 1 M HEPES buffer, 5 mL of 100x L-glutamine, 5 mL ITS media supplement, 5 mL of 100x penicillin-streptomycin, 2 mL of 250 µg/ml amphotericin-B, and 12 µL of 1 mM dexamethasone. Just prior to application onto cells, 10 µL of 10 µg/mL of interferon-γ (IFNγ) and 4 µL of 10 ng/mL epithelial growth factor (EGF) respectively were added per 10 mL medium. Cells were incubated at 33°C and 5% CO_2/95% humidified air.

Cell Dosing

Cells were seeded into either 6-well or 96-well collagen coated tissue culture plates depending on the required cell need for each experiment. All dosing was done at approximately 70% confluency in both cell lines, and doses comprised multiple concentrations of each compound added in completed medium. Specific doses of each compound for all experiments can be found in *Table 1*.

Table 1: Specification of all doses of each compound used in each experiment.

	Viability/*Gclm* Promotor Activity	**Total Glutathione**	**RNAseq**	**Lipid Peroxidation**
Formaldehyde	50 µM,100 µM, 150 µM, 200 µM, 250 µM, 400 µM, 500 µM	50 µM, 200 µM, 500 µM	N/A	50 µM, 200 µM
Acetaldehyde	100 nM, 1 µM, 10 µM, 100 µM, 1 mM	100 nM, 10 µM, 1 mM	N/A	1 µM, 1 mM

Cinnamaldehyde	10 µM, 100 µM, 250 µM, 500 µM, 750 µM, 1 mM	10 µM, 250 µM, 750 µM	10 µM, 100 µM	10 µM, 50 µM (KO), 100 µM (WT)
Diacetyl	10 µM, 100 µM, 250 µM, 500 µM, 750 µM,1 mM	10 µM, 250 µM, 1 mM	250 µM, 1 mM	250 µM, 1 mM

Cell Viability

Cell viability was assessed in 96-well plates using alamarBlue Cell Viability Reagent from Invitrogen (Eugene, OR) with an adapted assay protocol. In brief, cells were incubated with the alamarBlue reagent at 33 ℃ for 2 hours rather than 37 ℃ for 1-4 hours. See *Supplemental Figure 1* for a comparison of incubation temperatures and times. Fluorescence was measured using excitation/emission settings of 560nm/590nm respectively. Plates were read using a Spectramax i3X spectrophotometer (Molecular Devices, San Jose, CA) with Softmax Pro 7.0 software. See *Supplemental Protocol 1* for the full protocol.

Quantitation of Cell Number

Cells were indirectly quantified in order to standardize fluorescence readings of subsequent *Gclm* promotor activity assays. Directly after viability evaluation, cells were fixed by adding 4% paraformaldehyde directly into the dosed medium-alamarBlue mixture in each of the wells. The plate was allowed to incubate at 37 ℃ for 30 minutes for maximum fixation, after which cells were gently washed with phosphate buffered saline (PBS). A 2 µg/mL Hoechst 33258 nuclear stain solution was then added, and the plate was again incubated at 37 ℃ for 15

minutes in the dark. Fluorescence was then measured on the Spectramax i3X using excitation/emission settings of 350nm/460nm respectively. In some of the higher doses, the extent of cytotoxicity was such that a majority of the cells had lifted off the bottom of the wells. Subsequently they were not properly fixed, were washed away with the PBS, and were not counted when measuring Hoechst fluorescence which is why these measurements were only used to standardize *Gclm* promotor activity. See *Supplemental Protocol 1* for the full protocol.

Gclm Promotor Activity

Gclm promotor activity was measured using the fluorogenic compound 9H-(1,3-Dichloro-9,9-Dimethylacridin-2-One-7-yl) β-D-Galactopyranoside (DDAOG) in the *Gclm* knockout cells. When cleaved by β-galactosidase, DDAOG is converted to its aglycone DDAO which is fluorescent. In addition to the *Gclm* gene knockout, the cell line had a concurrent β-galactosidase/neomycin phosphotransferase knock-in, replacing exon 1. This allowed for the quantitation of *Gclm* promotor activity using DDAOG fluorescence as a proxy. These experiments were run in the same plates as the Hoechst staining. Residual Hoechst solution was moved from the cells, which were then washed with PBS. A 10 μM DDAOG solution was then added, and the plate was incubated for 20-24 hours at 4℃ in the dark. See *Supplemental Figure 2* for protocol optimization. The fluorescence was measured on the Spectramax i3X using excitation/emission settings of 633nm/670nm respectively. See *Supplemental Protocol 2* for the full protocol.

Total GSH Levels

Total glutathione levels were quantitated using a naphthalene-2-3-dicarboxaldehyde (NDA) assay. In brief, cells were plated, dosed, and subsequently lysed in 6-well plated in order to ensure enough cells for GSH detection. Lysates were transferred to 1.7 mL tubes and sonicated at 40 mA using two 5 second bursts in order to fully disrupt the cells. Part of the disrupted lysate was transferred to a new tube with an equal volume of 10% sulfosalicylic acid (Sigma-Aldrich, St. Louis, MO) in order to precipitate out any protein; this portion was centrifuged, and the supernatant removed to measure total GSH levels. The remaining disrupted lysate was used later for protein quantitation. Any oxidized GSH (GSSG) was reduced using tris(2-carboxyethyl)phosphine (TCEP) (Thermo-Fisher, Rockford, IL) at pH 7-8. Reduced GSH was then conjugated to NDA (Sigma-Aldrich, St. Louis, MO) at pH 12.5. Samples were added in triplicate to a black-walled, black-bottom 96-well plate, and fluorescence was measured on the Spectramax i3X using excitation and emission settings of 472nm/528nm. GSH levels were calculated by comparing sample fluorescence to the fluorescence generated by a set of serially diluted GSH standards, and readings were standardized by using sample protein levels as a denominator. See *Supplemental Protocol 3* for the full protocol.

RNAseq

Cells intended for RNAseq analyses were plated in 6-well plates to ensure enough RNA for valid readings. Dosing and cell lysis were also done in the same 6-well plate. RNA was extracted using the miRNeasy kit from Qiagen (Hilden, Germany). Samples were sent out and sequencing data was generated by BGI (Cambridge, MA). The raw reads were aligned to the mouse GRCm38.p6 transcriptome using the *Salmon* aligner.[10] The reads were then summarized at the gene level using the Bioconductor *tximport* package.[11] Principle component analysis was

run on the submitted samples to rule out potential confounding factors in dose or genotype differences (see *Supplemental Figure 3*). Pathway analysis was performed using iPathwayGuide (Advaita Bioinformatics, Ann Arbor, MI).

Lipid Peroxidation Levels

Lipid peroxidation levels were measured using the MDA assay kit from Sigma-Aldrich (St. Louis, MO) with the manufacturer's provided protocol. Cells were plated, dosed, and harvested in 6-well plates to ensure enough cells for peroxidized lipid detection. Lysates were transferred to 1.7 mL tubes and sonicated at 40 mA for two 5 second bursts in order to fully disrupt the cells. Samples were then centrifuged at 13000 x g for 10 minutes, after which 200 µL of the supernatant were transferred to a new tube; the remaining material was used for protein quantitation. Next, 600 µL of TBA solution were added to all tubes with the transferred supernatant, and the mixtures were allowed to incubate at 95 °C for 60 minutes in a heating block. Tubes were then inverted to mix, and 200 µL of each sample were added in triplicate to a black-walled, black-bottom 96-well plate. Fluorescence was measured on the Spectramax i3X using excitation and emission settings of 532nm/553nm. Sample concentrations were determined by comparing fluorescence values against a standard curve of MDA with known concentrations. See *Supplemental Protocol 4* for the full protocol.

Protein Quantitation

Protein quantitation for the standardization of total GSH levels and lipid peroxidation levels was carried out using protein dye supplied by Bio-Rad Labs Inc. with its associated

protocol. In brief, 10 µL of protein sample were added in triplicate to a clear-walled, clear-bottom 96-well plate. This was followed by the addition of 200 µL of protein dye, and plates were gently vortexed to ensure adequate mixing. The absorbance of each plate was then read at a wavelength of 595 nm on the Spectramax i3X. Sample concentrations were determined by comparing with standard protein solutions of known concentrations. See *Supplemental Protocol 5* for the full protocol.

Benchmark Dose (BMD) Range Determination

BMD ranges were calculated using the EPA's BMDS 3.1.1 software. Models were generated by inputting the viability data for each compound. The BMD was set to capture the dose at which each model's lower confidence bound showed a 10% change from the negative control ($BMDL_{10}$); all default models were created, and an approximate range of the $BMDL_{10}$ was created such that it encompassed a majority of the models while not being overly broad. See *Supplemental Figures 4-6* for the generated models.

Data Analyses

All data obtained from cell viability, *Gclm* promotor activity, total GSH, and lipid peroxidation experiments were statistically analyzed using Prism 8 software. For analyses examining responses in both cell lines, a 2-way ANOVA was run. To look at effects across doses, a Dunnett's multiple comparisons post-hoc analysis was run using each cell line's negative control as the comparison group; to look at genotype differences in the cell viability experiments, a Bonferroni multiple comparisons test was run. Because the *Gclm* promotor activity experiment only made use of the knockout line, data were analyzed using a 1-way

ANOVA with a Dunnett's T3 multiple comparisons post-hoc test. RNAseq group comparisons were made using the edgeR package, and were fitted using a quasi-likelihood negative binomial generalized linear model.[12] Quasi-likelihood F-tests were conducted for given coefficients or contrasts.[13] Statistical significance was determined by using Benjamini-Hochberg multiple comparison testing procedures with a false discovery rate (FDR) of 5%. Pathway analysis made use of the Impact Analysis method to determine relevant enriched pathways.[14,15,16]

Results:

Formaldehyde

Figure 1 details the effects of formaldehyde across all experiments performed. Formaldehyde elicited a prototypical dose-response relationship with respect to viability in both cell lines. The wild type line saw significant decreases in overall viability by 200 μM ($P = 0.01$), whereas the knockout line only showed statistically significant decreases at doses of 400 μM and above ($P < 0.001$). The knockout line showed significantly higher values than the wild type line at the 150 μM ($P = 0.03$) and 200 μM ($P = 0.02$) doses, but not at other doses. The rough $BMDL_{10}$ range for the wild type cells was 60 μM-80 μM, whereas for the knockout cells it was 140 μM-160 μM. *Gclm* promotor activity showed a slight initial induction at concentrations as low as 50 μM ($P = 0.01$). Doses between 100 μM and 250 μM showed no significant changes in promotor activity, however at 400 μM and above, promotor activity was drastically reduced. These trends appear to track with total GSH levels in the wild type cells. Despite a lack of significance ($P = 0.07$), cells at the lowest dose of 50 μM appeared to contain a greater amount of GSH. As the dose increased to 200 μM, cellular GSH levels appeared to drop back toward baseline levels or lower, though again there were no statistically significant decreases. TBARS

data contained much variability, and therefore showed no statistically significant alterations of lipid peroxidation levels when compared to baseline. The knockout cells appeared to display higher levels of peroxidized lipids at all dose levels, but again variability precluded any statistically significant differences between genotypes.

Acetaldehyde

Figure 2 details the effects of acetaldehyde across all experiments performed. Exposure to acetaldehyde had very little effect across all experiments in both cell lines. Interestingly, there was one dose that resulted in a statistically significant increase in cell viability, but only in wild type cells (1 μM, $P = 0.01$). Knockouts showed no significant deviations in viability in response to dose. Nor were there major differences in response between genotypes. Due to the lack of any significant negative changes in viability, no $BMDL_{10}$ was generated for acetaldehyde. In our model system, the $BMDL_{10}$ should be considered greater than the highest dose (1 mM). Though not significant for every dose, the induction of the *Gclm* promotor appears relatively sustained. Total GSH levels in the wild type cells show a significant decrease at the lower doses of 100 nM and 10 μM, with a less significant decrease at 1 mM ($P = <0.001, <0.001$, and 0.02 respectively). No significant differences were seen in knockout GSH levels. Similar to formaldehyde, there was much variability in the lipid peroxidation data. When looking on a per-dose basis there were no significant changes in lipid peroxidation. However, when the data was reanalyzed to compare dosed vs. undosed cells there was a significant genotype difference in the dosed cells (See *Supplemental Figure 7, P = 0.02*).

Cinnamaldehyde

Figure 3 details the effects of cinnamaldehyde across all experiments performed. Cinnamaldehyde had some of the greatest adverse effects across experiments. Wild type cell viability significantly decreased at both 750 μM and 1 mM ($P = 0.01$). Knockout viability showed both steep and significant decreases in viability at doses as low as 250 μM ($P < 0.001$). Interestingly, viability trended upwards between 250 μM and 750 μM but then dropped again at the highest dose of 1mM. Responses between genotypes were significantly different at 250 μM, 500 μM, and 1 mM ($P < 0.001$). There was no significant difference between genotype responses at 750 μM. The $BMDL_{10}$ range for the wild type cells was 150 μM-200 μM, and for the knockout cells it was 90 μM-110 μM. *Gclm* promotor activity showed a significant induction at 100 μM ($P = 0.03$), but again there was a steep decrease in activity at 250 μM ($P < 0.001$). There was no resurgence in promotor activity as seen in the viability curve. These results tell a somewhat different story when compared to total GSH levels. In the wild type cells, there was a significant decrease in GSH content at the lowest dose tested of 100 μM ($P < 0.001$). However, the decrease is also seen at the next highest dose of 250 μM ($P < 0.001$). The knockout cells show no significant changes in total GSH levels. Like the previous two compounds, lipid peroxidation levels were variable and did not demonstrate any statistical significance across compound dose or genotype. The trend of potentially higher baseline lipid peroxidation is once again seen, though differences at each of the two doses is less pronounced than the other two compounds described so far.

RNAseq data showed only two significant differentially expressed genes in wild type cells at 10μM cinnamaldehyde. Both were glutathione-S-transferase A (*Gsta*) and both were upregulated. At the 100 μM dose, 197 genes in wild type cells were shown to be differentially expressed with 169 genes upregulated and 28 genes downregulated. Because only two genes

were differentially expressed at the 10 μM dose, no pathway analysis was run at this level. However, 195 of the 197 differentially expressed genes from the 100 μM dosed wild type cells were run through pathway analysis. Of the five most impacted pathways, the majority involved drug and xenobiotic metabolism. Unsurprisingly there was a general upregulation of multiple GSTs, though there was also a concomitant upregulation of multiple UDP-glucuronosyltransferases (UGTs). See *Figure 5* for a list of the top five impacted pathways and corresponding partial gene expression profile for the top impacted pathway.

RNAseq revealed a similarly low number of differentially expressed genes in the knockout cells at 10 μM cinnamaldehyde, however in this case there were zero genes with altered expression when compared to baseline. There were unfortunately no 100 μM samples run for the knockout cells due to unforeseen cytotoxicity issues across all three replicates. Therefore, there was no pathway analysis run for any of the cinnamaldehyde knockout cells in the context of a baseline comparison.

We also ran pathway analysis to compare differential expression between the wild type and knockout cells at the 10 μM dose. Since there were little to no differentially expressed genes at this dose level in both lines, these results are almost identical to baseline gene expression comparisons. To put it another way, there were 7506 genes with significant expression differences when comparing the genotypes at the 10 μM dose level; however, when comparing how they deviate from their baseline gene expression patterns, there were zero significant genes.

Diacetyl

Figure 4 details the effects of diacetyl across all experiments performed. Looking explicitly at viability, diacetyl appears to have little effect on both cell lines. There were no

statistically significant deviations from baseline in the wild types except at the 1 mM dose ($P < 0.001$). The knockout cells showed no significant decreases in viability across all doses tested. The knockouts appeared slightly more resilient at the highest dose, though the result only approached significance ($P = 0.09$). The BMD_{10} range for the wild type cells was 220 μM-260 μM; since there were no significant decreases in viability in the knockout cells, no $BMDL_{10}$ range was generated and in our model system the BMDL10 should be considered greater than the highest dose (1 mM). *Gclm* promotor activity showed no significant deviations from baseline, but the data trended higher than the negative control across all doses. Total GSH levels initially decreased at the lowest dose tested of 10 μM ($P = 0.04$), but increased above baseline levels at the next highest dose tested of 250 μM ($P = 0.04$). The levels were further increased at 1 mM ($P < 0.001$). Lipid peroxidation levels demonstrated, as in all other compounds, large variability and no statistical significance among any of the diacetyl doses. The characteristic of knockout cells having higher overall levels of peroxidized lipids is repeated for a fourth time.

RNAseq data revealed no differentially expressed genes in the wild type cells at a dose of 250 μM diacetyl. However, at a 1 mM dose there were 6326 genes with significant expression differences from baseline; 2696 genes were upregulated, and 3630 genes were downregulated. Pathway analysis was used to probe the 1 mM gene expression changes, but due to the large number of differentially expressed genes a logFC threshold of +/-1.0 was applied to focus the results down to between 1000-2000 genes. This resulted in 1065 genes considered in the analysis. Many of the biological functions and molecular pathways impacted were related to various metabolic processes (fatty acid and pyruvate metabolism were the top two) and biosynthetic processes (steroid/cholesterol synthesis predominated). The vast majority of the genes comprising these processes were shown to be downregulated. Impacts on xenobiotic

metabolism ranked tenth, though in contrast to the metabolic and biosynthetic pathways many of these involved genes were upregulated. *Gclm*, as well as various Phase I and II related genes such as *Gst*s, *UGT*s, and carbonyl reductases (*Cbr*s) were upregulated. See *Figure 6* for the list of the top five impacted pathways and corresponding partial gene expression profile for the top impacted pathway.

In 250 μM dosed *Gclm* knockout cells, RNAseq showed 1437 total genes were differentially expressed when compared to baseline, with 326 genes upregulated and 1111 genes downregulated. Pathway analysis at this dose identified relatively unspecific impacts on binding, such as cell-cell and cell-extracellular matrix interactions. The analysis did also reveal various perturbations in signaling systems. Growth factor signaling ranked ninth in terms of affected molecular functions. For 1 mM dosed *Gclm* knockout cells, 9003 genes had significant differential expression when compared to baseline; 3876 genes were upregulated, and 5127 genes were downregulated. Again, due to the large number of genes available for comparison with pathway analysis, a logFC threshold of +/-1.32 was applied to narrow the scope of the analyses down to between 1000-2000 genes. In total, 1599 genes met this criterion and were included. Perturbations in binding and receptor interactions were still seen as with the lower dose level. Signaling pathways were also altered—specifically with respect to cytokines and chemokines. This was in addition to perturbations in steroid biosynthesis and energy metabolism—which were also seen in the wild type cells at this dose. There were also gene expression changes associated in very different processes including ATP binding cassette (ABC) transporters and calcium binding. *Figures 7* and *8* summarize the transcriptomic comparisons (dose vs. negative control) in the knockout cells at 250 μM and 1 mM respectively.

Much like with cinnamaldehyde, we ran pathway analysis to look at the differences in expression between the two cell lines at both doses. At 250 μM diacetyl, there were 7850 genes with significantly different expression levels. In the context of knockout cells versus wild type cells, 3827 genes were comparatively upregulated and 4023 were comparatively downregulated. There were no significant differences in how each cell line deviated from its baseline expression patterns. At 1 mM diacetyl, there were 8063 differentially expressed genes between cell lines. Again, in the context of knockout cells versus wild type cells, there were 3642 comparatively upregulated genes and 4421 comparatively downregulated genes. In this instance, when comparing deviations from baseline expression, 4451 genes were statistically significant; to focus the results of this pathway analysis, a logFC threshold of +/-1.0 was applied to reduce the number of genes under scrutiny to 1000-2000.

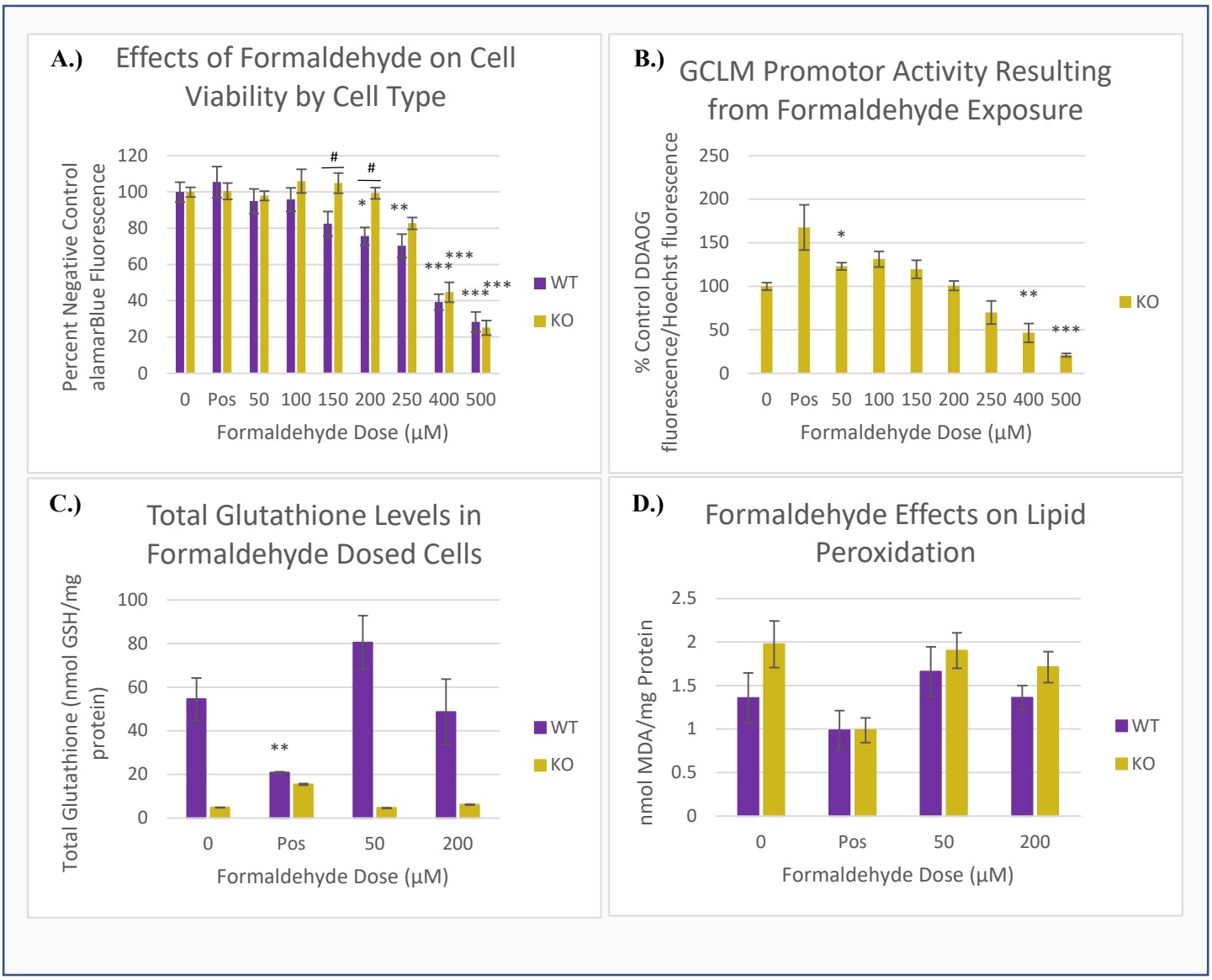

Figure 1: **A.)** Dose dependent effects of formaldehyde exposure on both the wild type (purple bars) and knockout (gold bars) cell lines. **B.)** Dose dependent effects of formaldehyde exposure on *Gclm* promotor activity as measured in knockout cells. Due to the replacement of the *Gclm* gene with a β-galactosidase gene, promotor activity was measured using β-galactosidase expression as a proxy. **C.)** Dose dependent effects of formaldehyde exposure on total glutathione levels in wild type and knockout cells. **D.)** Dose dependent effects of formaldehyde exposure on lipid peroxidation levels. Data for all plots are presented as the mean +/- SEM

Dose significance: * = $0.01 \leq P < 0.05$; ** = $0.001 \leq P < 0.01$; *** = $P < 0.001$

Genotype significance: # = $0.01 \leq P < 0.05$; ## = $0.001 \leq P < 0.01$; ### = $P < 0.001$

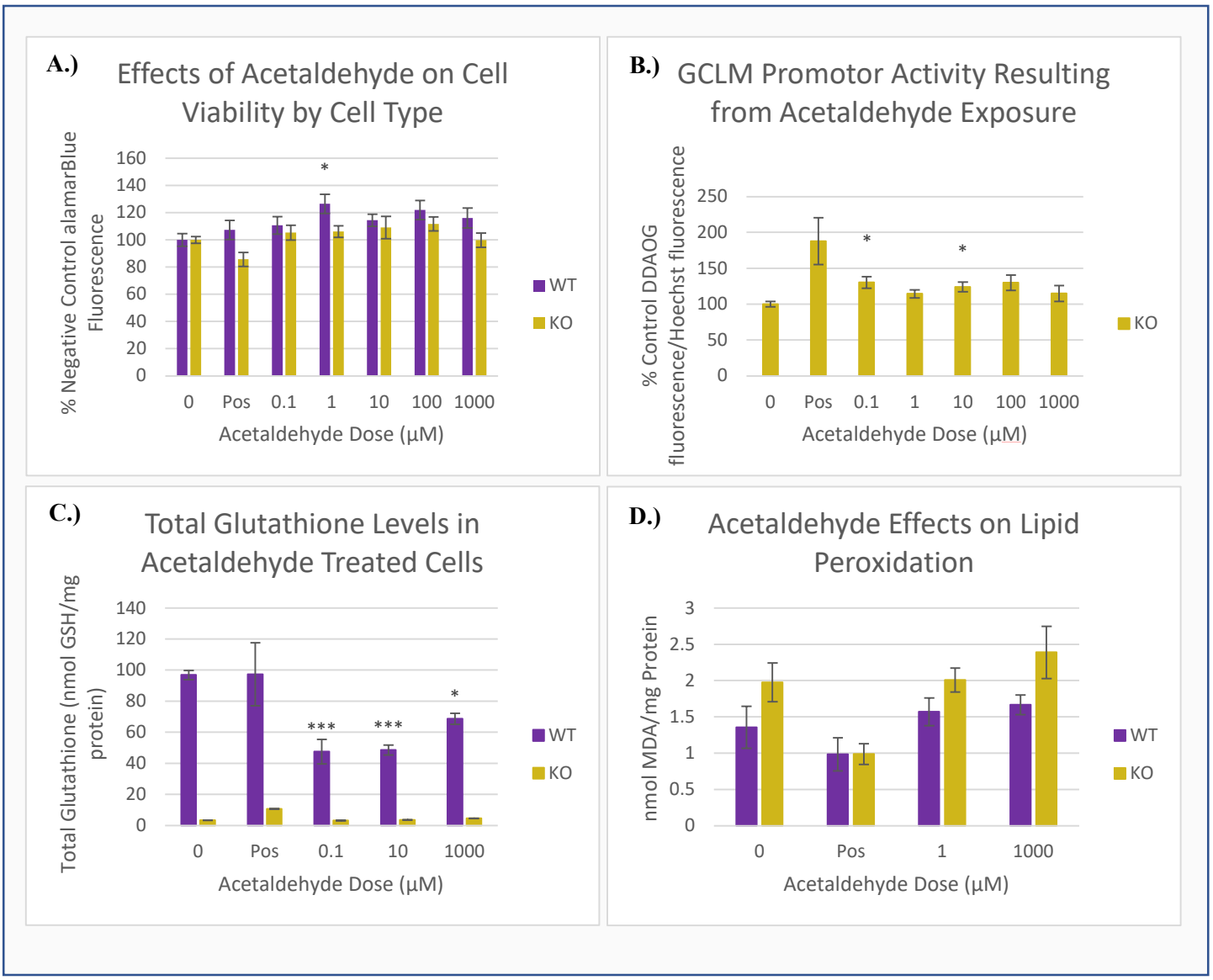

Figure 2: **A.)** Dose dependent effects of acetaldehyde exposure on both the wild type (purple bars) and knockout (gold bars) cell lines. **B.)** Dose dependent effects of acetaldehyde exposure on *Gclm* promotor activity as measured in knockout cells. Due to the replacement of the *Gclm* gene with a β-galactosidase gene, promotor activity was measured using β-galactosidase expression as a proxy. **C.)** Dose dependent effects of acetaldehyde exposure on total glutathione levels in wild type and knockout cells. **D.)** Dose dependent effects of acetaldehyde exposure on lipid peroxidation levels. Data for all plots are presented as the mean +/- SEM

* = $0.01 \leq P < 0.05$; ** = $0.001 \leq P < 0.01$; *** = $P < 0.001$

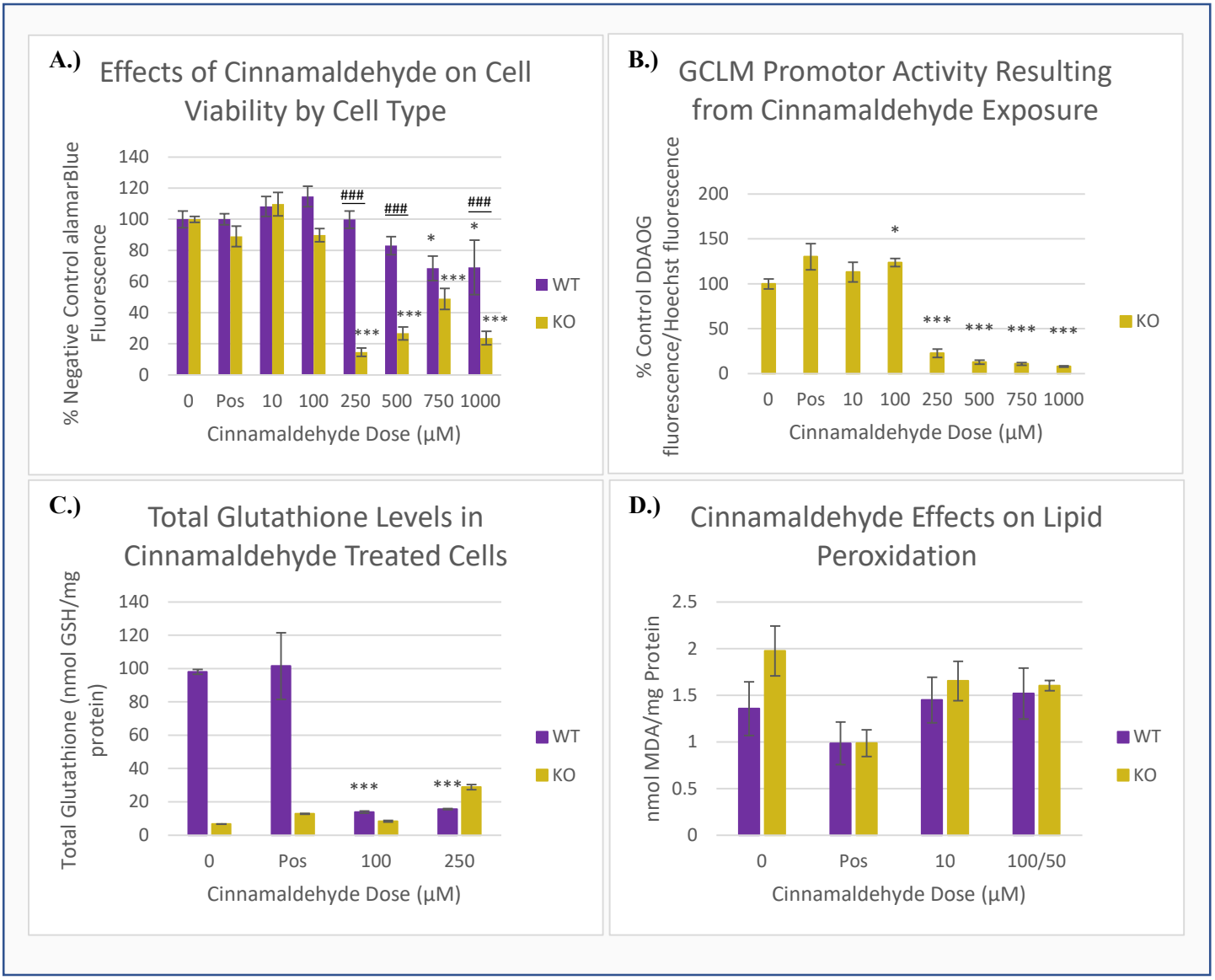

Figure 3: **A.)** Dose dependent effects of cinnamaldehyde exposure on both the wild type (purple bars) and knockout (gold bars) cell lines. **B.)** Dose dependent effects of cinnamaldehyde exposure on *Gclm* promotor activity as measured in knockout cells. Due to the replacement of the *Gclm* gene with a β-galactosidase gene, promotor activity was measured using β-galactosidase expression as a proxy. **C.)** Dose dependent effects of cinnamaldehyde exposure on total glutathione levels in wild type and knockout cells. **D.)** Dose dependent effects of cinnamaldehyde exposure on lipid peroxidation levels. Data for all plots are presented as the mean +/- SEM

Dose significance: * = $0.01 \leq P < 0.05$; ** = $0.001 \leq P < 0.01$; *** = $P < 0.001$

Genotype significance: # = $0.01 \leq P < 0.05$; ## = $0.001 \leq P < 0.01$; ### = $P < 0.001$

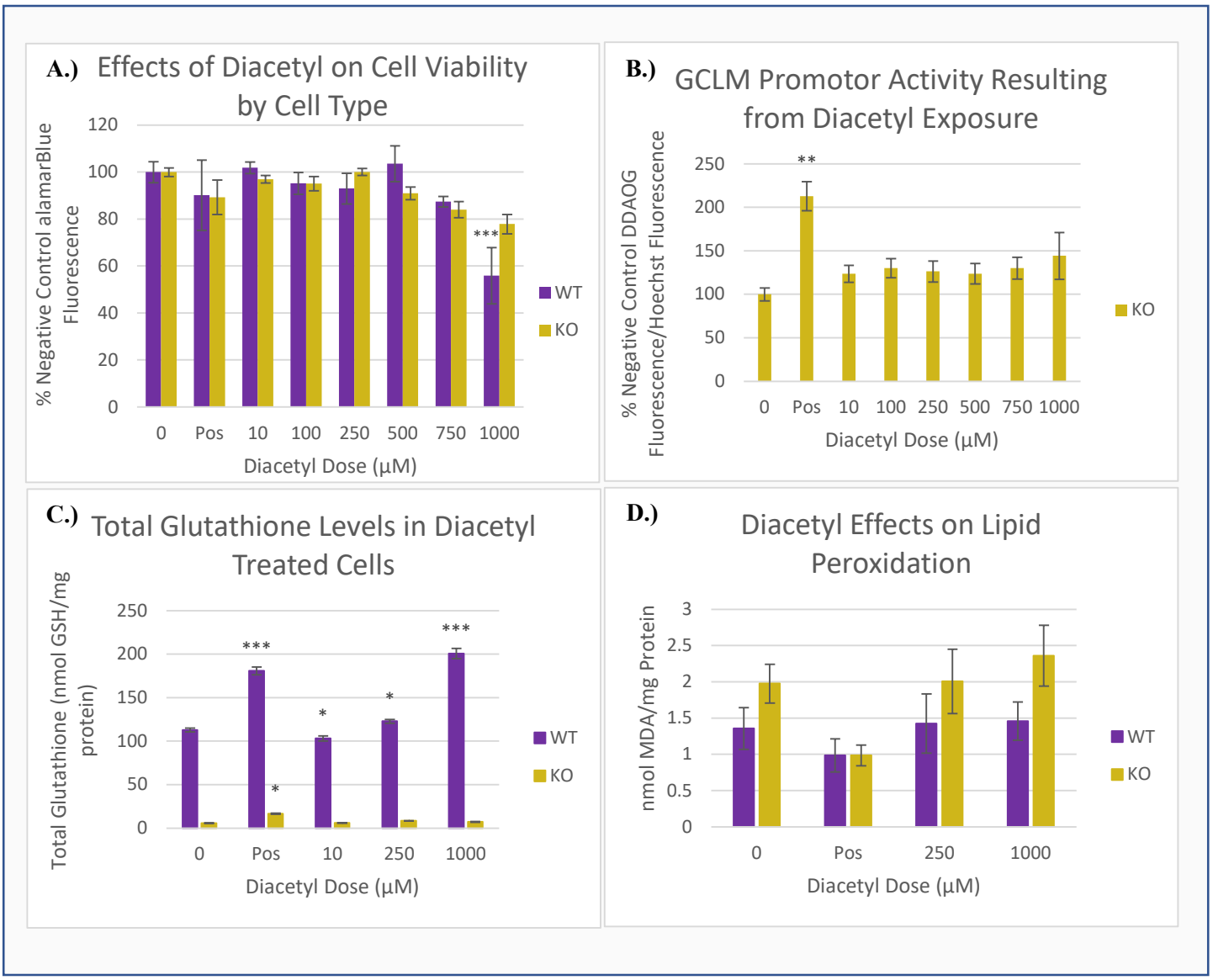

Figure 4: **A.)** Dose dependent effects of diacetyl exposure on both the wild type (purple bars) and knockout (gold bars) cell lines. **B.)** Dose dependent effects of diacetyl exposure on *Gclm* promotor activity as measured in knockout cells. Due to the replacement of the *Gclm* gene with a β-galactosidase gene, promotor activity was measured using β-galactosidase expression as a proxy. **C.)** Dose dependent effects of diacetyl exposure on total glutathione levels in wild type and knockout cells. **D.)** Dose dependent effects of diacetyl exposure on lipid peroxidation levels. Data for all plots are presented as the mean +/- SEM
* = $0.01 \leq P < 0.05$; ** = $0.001 \leq P < 0.01$; *** = $P < 0.001$

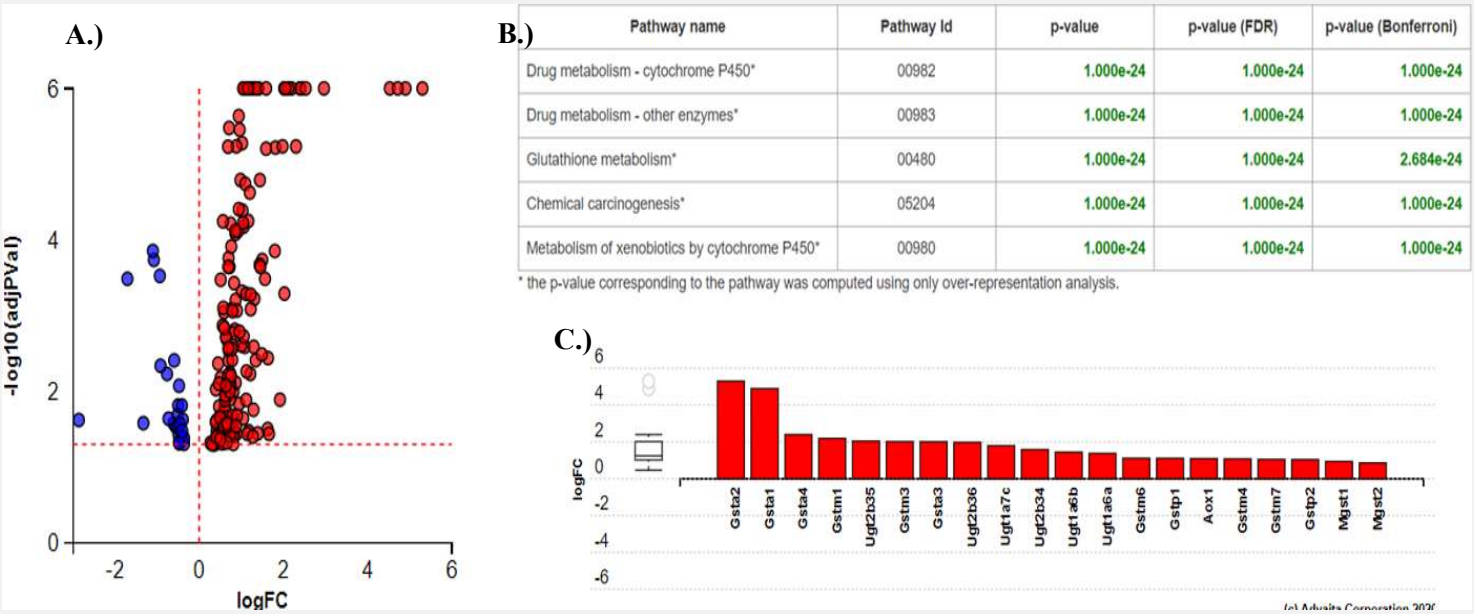

Figure 5: Summary transcriptomic data for 100µM cinnamaldehyde dosed *Gclm* wild type cells **A.)** A volcano plot showing the number of differentially upregulated (red dots) and downregulated (blue dots) genes. **B.)** The top five predicted impacted pathways according to pathway analysis. **C.)** A partial representation of the relative gene expression of the top impacted pathway (Drug metabolism – cytochrome P450); red bars denote upregulated genes, and blue bars represent downregulated genes.

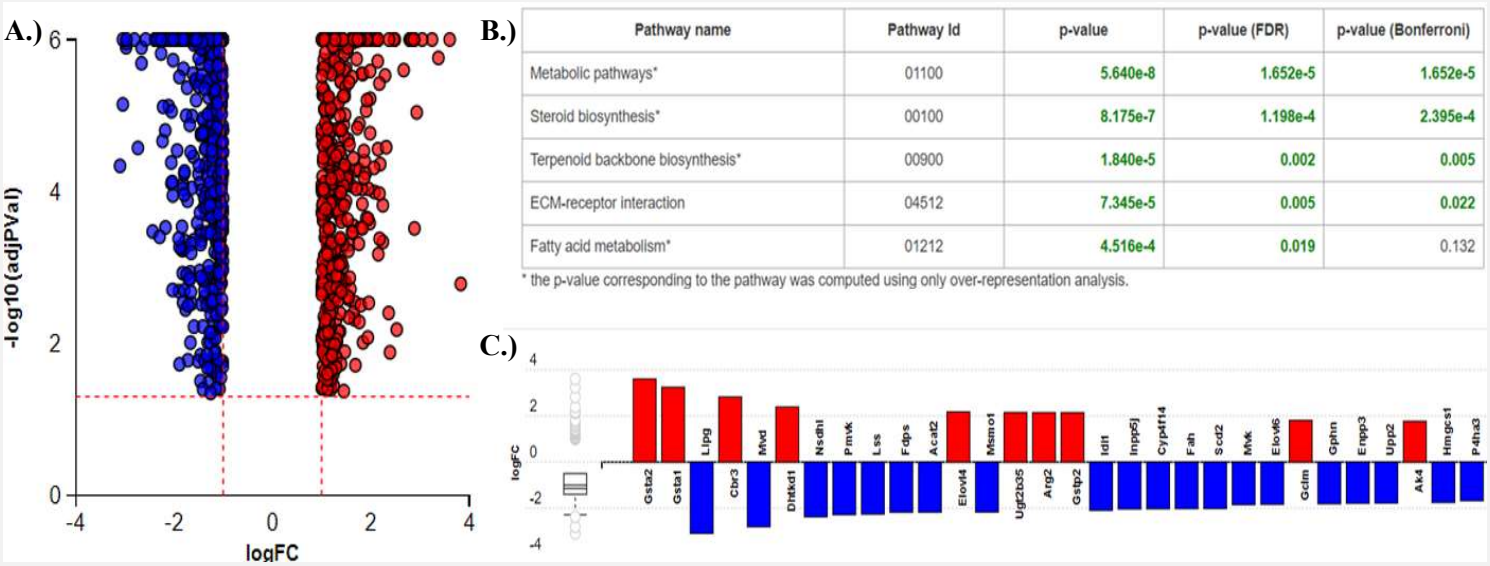

Figure 6: Summary transcriptomic data for 1mM diacetyl dosed *Gclm* wild type cells **A.)** A volcano plot showing the number of differentially upregulated (red dots) and downregulated (blue dots) genes. **B.)** The top five predicted impacted pathways according to pathway analysis. **C.)** A partial representation of the relative gene expression of the top impacted pathway (Metabolic pathways); red bars denote upregulated genes, and blue bars represent downregulated genes.

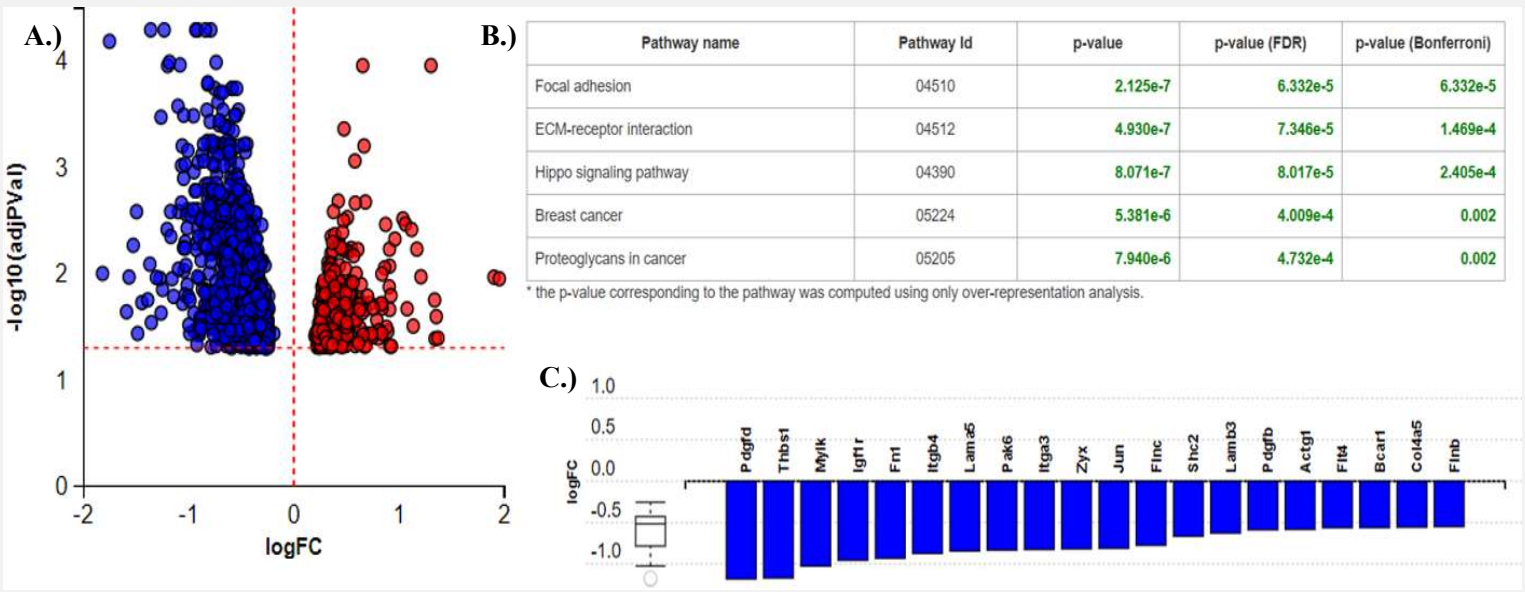

Figure 7: Summary transcriptomic data for 250µM diacetyl dosed *Gclm* knockout cells **A.)** A volcano plot showing the number of differentially upregulated (red dots) and downregulated (blue dots) genes. **B.)** The top five predicted impacted pathways according to pathway analysis. **C.)** A partial representation of the relative gene expression of the top impacted pathway (Focal adhesion); red bars denote upregulated genes, and blue bars represent downregulated genes.

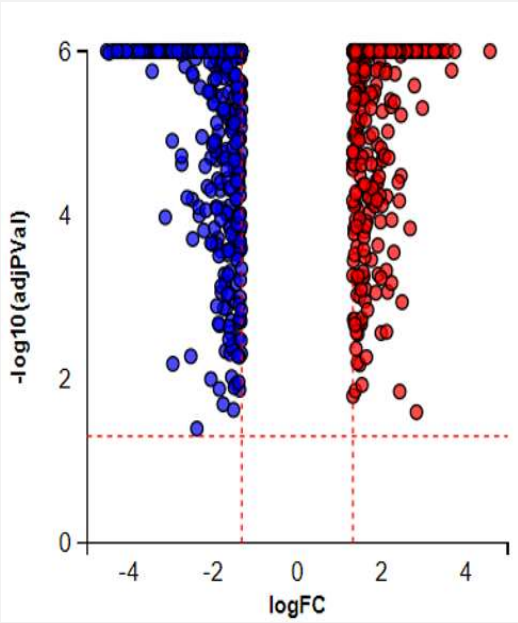

Pathway name	Pathway Id	p-value	p-value (FDR)	p-value (Bonferroni)
ECM-receptor interaction	04512	2.342e-5	0.004	0.007
Steroid biosynthesis*	00100	2.476e-5	0.004	0.008
Cytokine-cytokine receptor interaction	04060	5.990e-5	0.005	0.019
Metabolic pathways*	01100	6.413e-5	0.005	0.020
Peroxisome*	04146	6.332e-4	0.040	0.199

* the p-value corresponding to the pathway was computed using only over-representation analysis.

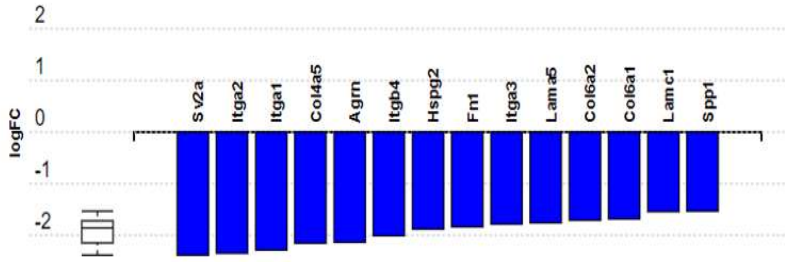

Figure 8: Summary transcriptomic data for 1mM diacetyl dosed *Gclm* knockout cells **A.)** A volcano plot showing the number of differentially upregulated (red dots) and downregulated (blue dots) genes. **B.)** The top five predicted impacted pathways according to pathway analysis. **C.)** A partial representation of the relative gene expression of the top impacted pathway (ECM-receptor interaction); red bars denote upregulated genes, and blue bars represent downregulated genes.

Discussion:

A large body of the current literature around e-cigarettes focuses on evaluating cellular and physiological responses to bulk vaping liquids. While this provides extremely useful insights, there are massive amounts of variability innate to vaping. There is currently very little regulation as to what compounds can be included in formulations, and the formulations themselves often contain multiple components. A large proportion of many vaping liquids consists of a mixture of propylene glycol and vegetable glycerin acting as humectants, which can give rise to pyrolysis byproducts such as formaldehyde, acetaldehyde, and acrolein.[17] Additionally, the legalization of cannabis in some states has opened up the industry to develop completely different formulations containing THC and other cannabinoids, as well as to cutting agents. Other variability to account for when examining health effects in bulk vaping liquids is the temperature of pyrolysis. Alterations in battery output, heating element resistance, and the chosen wicking material can all change the temperature at which the compounds in the base liquid are heated.[1] In fact, one study found that peak heating coil temperatures in certain kinds of e-cigarettes could vary from 110 ℃-1008 ℃ depending on those parameters.[18] Different heating temperatures can then influence the proportion and quantity of different reactive carbonyl by-products formed, with higher voltage outputs tending to produce higher amounts of by-products.[19,33] These facets make the generalizability of these effects across all formulations difficult due to the multiple potential sources of confounding.

This study takes a different approach to addressing the issue of vaping hazards. Rather than looking at the bulk vaping liquids, four specific compounds commonly associated with vaping were chosen and applied to immortalized mouse hepatocytes. Formaldehyde and acetaldehyde were chosen as pyrolysis by-products of the humectants in many of the

formulations on the market, and cinnamaldehyde and diacetyl were chosen as readily found flavoring agents. This approach allows the parsing out of compound-specific dose-response effects, and eliminates some of the confounding factors seen when working with bulk liquids. However, it would be remiss to omit the fact that this approach is not able to capture any synergistic or antagonistic effects that the compounds can potentially exert on one another when combined. Nor does this study design provide any indication of potential effects of chronic exposure, which would be very helpful in any risk assessments given the habitual nature of vaping. What this approach can be used for is to provide guidance on what compounds should be investigated further in more comprehensive model systems, or preliminarily identify compounds that should not be included in vaping liquid formulations.

Given the nature of vaping, much of the research currently undertaken focuses on the lungs. This study appears to be one of the few that looks specifically at effects on the liver, specifically with relation to how GSH plays a role in altering said effects. Focusing on the liver may seem counter-intuitive considering that vaping, by definition, involves respiratory exposures. However, given the anatomy and physiology of the lungs it serves to reason that some proportion of any inhaled compounds will be absorbed across the thin alveolar lining and cross into the blood, whereby they could be taken to the liver to be metabolized and biotransformed to aid in excretion. In fact, potential links between vaping and liver effects have been demonstrated in other studies. Notably, nicotine containing vaping products have been shown to potentiate lipid accumulation and oxidative stress in ApoE-/- mice on a concurrent Western diet.[25] A follow-up study in the same mouse model revealed that nicotine containing vaping liquids also resulted in increased levels of hepatic DNA damage and mitochondrial dysfunction, in addition to providing further evidence of increased reactive oxygen species generation.[48] Yet another

study focusing on the effects of nicotine found increased hepatic fibrosis in CD-1 mice chronically exposed to nicotine containing e-cigarette vapors; however, in this case the damage appeared indirect and was likely tied to increases in systemic inflammatory signals.[49] Additionally, elevated liver values and increased levels of oxidative stress were found in a study consisting of rats injected intra-peritoneally with vaping liquid with and without nicotine.[38] Considering the role the liver plays in metabolism and xenobiotic detoxification, any potentially harmful outcomes should be examined in detail.

It appears that formaldehyde exerts a prototypical dose response effect in the context of overall cell viability. Interestingly, the knockouts appeared slightly more resilient to exposure. Despite only achieving statistical significance at 150 and 200 μM, the knockouts consistently appeared to have higher relative viability at all doses except the highest. Unsurprisingly, the predicted $BMDL_{10}$ ranges of each cell line supports this idea. The knockout cells had a $BMDL_{10}$ about twice as high as that of wild type cells. When looking at how formaldehyde exposure impacts GSH formation and use, the results also appear reasonably expected. At low doses, the *Gclm* promotor shows mild to moderate induction, suggesting an initial antioxidant response. By the highest two doses, promotor activation (and presumably the ability of Nrf2 or other trans-activators to bind to it) drops to very low levels. This pattern is somewhat mirrored in the GSH quantitation data. At the lowest dose GSH levels appear elevated (approaching significance, $P = 0.065$), and by mid-range doses the levels have dropped back to near or below baseline. Taken together, these data show that GSH does play a role in detoxifying formaldehyde, but also that antioxidant systems begin to become overwhelmed by around 100-200 μM. However, the fact that the *Gclm* knockout cells appear more resistant indicates that a compensatory pathway upregulated in these cells may provide greater protection. Unfortunately, there is no RNAseq

data for formaldehyde exposure, so any conjecture would have to be based upon basal differences between the two lines. Given the multiple upregulated UGTs, it is possible that glucuronidation may contribute to the protection in the *Gclm* knockout cells. This seemingly counter-intuitive result has been demonstrated previously. For example, in a study examining the effects of pulmonary ozone exposures, *Gclm* null mice were more resistant to damage; it was found that those mice had increased expression of metallothioneines and other antioxidant coding mRNAs compared to their *Gclm* wild type counterparts.[50] This demonstrates that alternate antioxidant pathways are—at the very least—potentially more inducible in the context of a *Gclm* knockout genotype. Many of the significantly altered pathways in our untreated cell lines involve intracellular signaling or receptor-mediated signaling; many of the receptors and signal mediators appear more lowly expressed in the knockout cells, so dampened signaling responses could also contribute to knockout cell resilience. It should be noted that although the *Gclm* knockout cells appeared more resistant to formaldehyde induced cytotoxicity, they tended to have higher levels of peroxidized lipids. Even though there was no statistical significance for any of the doses, the trend was consistent across every compound tested. Conceptually this makes sense because GSH plays a key role of removing various reactive oxygen species, which are in turn responsible for peroxidizing lipids.

Formaldehyde appears to be readily absorbed by the body, but also readily metabolized by red blood cells.[46] Blood levels of formaldehyde are only lowly elevated compared to baseline when exposed to levels as low as 1.9 ppm (2.77 µg/g blood vs 2.61 µg/g blood).[46] However, formaldehyde concentrations found in vaping aerosols have been measured at up to 99.4 mg/m^3 (~81 ppm), which is above ACGIH's recommended exposure limit for formaldehyde, which is 0.37 mg/m^3 (0.3 ppm).[17] This does not take into account variability attributable to altering e-

cigarette parameters such as battery output or heating coil resistance. This already indicates vaping related formaldehyde exposures can be an issue. The question now becomes how these potential exposures may translate to impacting the liver. Increased DNA damage, lipid peroxidation, and protein oxidation have been measured in both liver and blood (lymphocytes) in rats exposed to as little as 10 ppm formaldehyde;[45] so even if the doses tested in this study may not be entirely true-to-life, the effects of formaldehyde should still be considered given the potential levels of exposures.

Acetaldehyde appeared to have the fewest obvious effects on both cell lines across each experiment. When looking at overall viability, all doses had either no significant effect, or resulted in increased viability in the case of the 1 μM dosed *Gclm* wild type cells. The lack of any significant differences between genotypes indicates that both cell lines have similar sensitivity. The viability results were mirrored when looking at *Gclm* promotor activity—all doses either showed no deviation from baseline or increased activity. Total GSH levels also provide additional evidence that GSH appears not to play a key role in acetaldehyde detoxification. Despite initial decreases at lower doses, GSH levels begin to return towards baseline levels at the highest dose, suggesting that the antioxidant response is adequately able to keep up with the exposure. Much like with formaldehyde, no significant changes in peroxidized lipids were seen across any doses, and the *Gclm* knockout cells tended to have higher though non-significant levels.

Given the scope of this study, it is unknown if the lack of negative effects is actually a result of acetaldehyde, or if it is instead due to its metabolism by-product acetate. Acetate is an important factor in energy metabolism, and the conversion of acetaldehyde to acetate by aldehyde dehydrogenase (ADH) may be providing positive trophic effects to the exposed cells.

This raises the issue of the potential for ADH polymorphisms increasing vapers' sensitivities to the e-liquids. Much of the current literature evaluates acetaldehyde exposure in the context of alcohol consumption; in this context ADH polymorphisms play a large role in how much acetaldehyde can be converted to acetate in the liver.[42] A study by Teeguarden et al developed a physiologically based pharmacokinetic (PBPK) model to try and estimate the extent of inhalation-based acetaldehyde exposures; the one drawback for this study is the fact that the PBPK model estimates respiratory tissue concentrations and does not translate it further into blood concentrations.[41] The model predicted linear increases from 0-6 mM in nasal epithelium acetaldehyde concentration with increasing air concentrations from 0-1000 ppm, and they found that ADH polymorphisms had little influence on max metabolic rates in these tissues.[41] To put this level in perspective, some vaped e-liquid formulations have been measured releasing up to 20.4 mg/m^3 (11 ppm)[17], though this does not take into account altered heating temperatures or battery outputs.

Cinnamaldehyde had some of the more interesting results out of the four compounds tested. It had the strongest negative effects on cell viability in the *Gclm* knockout cells, while having a much lesser impact on *Gclm* wild type cells. At all doses above 100 μM, the *Gclm* knockout cells were shown to be significantly less resilient. This is further confirmed when comparing their respective $BMDL_{10}$—with the *Gclm* knockout value being about twice as low as the *Gclm* wild type value. There was also a curious resurgence in viability in the *Gclm* knockout cells between 250 μM and 750 μM which is not able to be explained by the data at this time. These data match reasonably well with other studies on cinnamaldehyde and vaping, with noticeable viability effects at dose ranges of 3 μM (pulmonary fibroblasts)[26] all the way up to 5-10 mM (alveolar macrophages)[27]. In primary hepatocyte models, cinnamaldehyde cytotoxicity

can be seen at around 1 mM.[28] Examination of cinnamaldehyde's effects on glutathione provides good insights into potential mechanisms of this toxicity. Our data show an initial elevation in *Gclm* promotor activity by 100 μM and then a drastic decrease to around 20% of baseline by 250 μM. Despite these values being measured by proxy in the knockout cells, RNAseq data in the wild type cells recapitulates the fact that *Gclm* levels are in fact elevated at 100 μM. Despite the initial elevation in *Gclm*, quantitation of total GSH tells a different story. Even at 100 μM, GSH is severely depleted—down to about 15-20% of baseline. Taken together, these data strongly suggest antioxidant overload by concentrations as low as 100 μM (or possibly lower). A previous study in primary mouse hepatocytes demonstrated significant GSH depletion—and subsequent repletion—at doses between 50-500 μM, although the experiment only examined cells up to a maximum six hours after dosing.[28] It is also interesting that even the upregulation of other metabolic pathways was not enough to lessen the damage caused by cinnamaldehyde. RNAseq date in the wild type cells at 100 μM showed upregulation of genes involved in glucuronate formation and glucuronidation, as well as genes involved in general aldehyde metabolism such as aldehyde dehydrogenase, aldehyde oxidase, and aldoketoreductase.[30] Despite this, cytotoxicity and GSH depletion still occurred rapidly. This brings two potential consequences to mind. The first is that, even in GSH sufficient individuals, vaping cinnamaldehyde while exposed to other toxicants could exacerbate any negative effects due to the overload of the antioxidant system. The second consequence drawn from the data is that we would hypothesize that individuals with chronically low GSH levels are more at risk of harmful effects given the apparently key role that GSH plays in detoxifying this compound. The frequency that cinnamaldehyde seems to be found in various vaping liquids is worrying given these conclusions and requires further research.

To date, there are few to no studies examining the absorption and distribution of cinnamaldehyde given an inhalation exposure, meaning it is unknown how close to physiologically relevant the doses picked for this study are. Another study examining effects of cinnamaldehyde with respect to vaping used a maximal dose of 15 mM in bronchial epithelial cells.[27] The dose ranges chosen for this study were at least ten times lower to account for the lower concentrations likely seen by the liver when compared to the lung. *In vivo* studies shed some light on the issue, but there are still distinct data gaps. One such study by Zhao et al measured maximal blood concentrations of cinnamaldehyde of 82-249 ng/mL (0.62 μM-1.9 μM) given oral exposures of 125-500 mg/kg.[40] Given the differences in absorption properties between the lungs and the intestines, it can be reasonably assumed that blood concentrations will likely be higher when exposed via an inhalation route. Additionally, the high concentrations in some vaping liquid formulations could also make higher blood concentrations feasible. Multiple studies have shown that liquids containing cinnamaldehyde can have concentrations ranging from as low as 17 μM[26] to as high as 1 M or greater.[26,27,29] Given that some of the effects seen in this study were seen by doses as low as 100-250 μM it is well within the realm of possibility that vaping relevant concentrations may elicit some of these responses.

Much like cinnamaldehyde, diacetyl also presented unexpected results—but of a different nature. The compound gained its notoriety when it was linked to the development of bronchiolitis obliterans in microwave popcorn factory workers (hence the colloquial terminology "popcorn lung"). In humans, exposure in these workers resulted in a symptomology including cough, shortness of breath, wheeze, and general airway obstruction.[31] In the liver model used in this experiment, there were actually very little effects on overall cell viability in both cell lines. Wild type cells only demonstrated decreased viability at the highest dose (1 mM). Interestingly,

at this dose the knockout once again demonstrated greater viability, though this may not tell the whole story. There were no significant differences seen between genotypes. In both lines, overall cell health appeared unaffected upon visual examination—even at the 1 mM dose that appeared to negatively impact the wild type cells. Instead, it appeared there were lower levels of cell growth. In other words, diacetyl appeared to exert its effects through cytostatic mechanisms rather than cytotoxic mechanisms. This idea is further supported when taking the total protein data obtained across the different experiments run. Protein levels in samples with the highest dose of diacetyl tended to be 1.5-2 times lower than smaller doses in both cell lines (data not shown). None of the doses tested showed any significant change in *Gclm* promotor activity; total GSH levels showed initial depletion at the lowest dose, but at higher doses increased to above baseline. This suggests GSH may play some minor role in metabolizing and detoxifying diacetyl, but could be overshadowed by some other pathway. This could also explain the relative similarity in the cytotoxicity data between wild type and knockout cell lines. However, RNAseq analysis revealed that wild type cells experienced downregulation of multiple pathways related to energy metabolism and alterations in steroid and fatty acid biosynthesis. Knockout cells also demonstrated similar impacts on energy metabolism and steroid biosynthesis. A big difference is the fact that, although only approaching statistical significance, ABC transporters and calcium signaling also appear somewhat affected. Unfortunately, the scope of this project did not allow for the investigation of how these alterations could translate into notable effects but would be interesting to investigate in future experiments. As it stands, diacetyl's mechanism of action on wild type cells may involve the depression of energy metabolism and other systems required for cell growth. This would help explain the lack of overt cytotoxicity coupled with the slower growth rates and lack of GSH depletion seen in those cells. Knockout cells, while also having

some of the same effects may also have to contend with dysregulated intracellular signaling (due to altered calcium-dependent pathways) and influx/efflux imbalances (due to altered transporter expression).

Unlike with cinnamaldehyde, the doses of diacetyl used in this experiment are likely less physiologically relevant. In a survey of multiple vaping liquids, one study measured diacetyl at a maximum level of 239 μg/e-cigarette; making the assumption that a typical e-cigarette contains 1mL of liquid, that would equate to approximately 3mM.[32] Few studies have looked in depth at the kinetics of diacetyl, and the ones that do exist typically focus on the different aspects of the respiratory system and stop there. One study in particular used a hybrid computational fluid dynamics-physiologically based pharmacokinetic model to estimate diacetyl exposures in the respiratory tract. The study found that in a human setting and with local metabolism taken into account, bronchiolar concentrations of diacetyl were estimated to be around 0.014 μM-0.08 μM via a mouth-breathing exposure pathway (depending on at rest or light exercise conditions) at 1 ppm, which was around the maximal concentration of diacetyl (3.69 $\mu g/m^3$) measured within twenty six formulations.[39,17] There was no indication of how much diacetyl would partition in the blood, but levels would likely be equivalent or lower. It should also be noted that there are many other formulations that have not been tested with higher diacetyl levels. Future studies examining the absorption and transport of diacetyl throughout the body via a respiratory exposure route would be greatly helpful in defining more physiologic *in vitro* experimental setups for non-lung model systems.

As a final remark, the seemingly counter-intuitive results presented in the lipid peroxidation should be addressed. Across all experiments, the hydroquinone positive controls exhibited lower levels of peroxidized lipids than the negative control counterparts. This is

surprising given the nature of hydroquinone; the compound can undergo multiple oxidation steps to form a semi-quinone or quinone which, and as a result can facilitate the production reactive oxygen species.[51] Lipid peroxidation then arises due to lipid interaction with those reactive oxygen species. Therefore, one would expect the cells treated with hydroquinone would have higher levels of peroxidized lipids than negative controls. Our results could potentially be explained in a number of ways, including the idea that reactive oxygen species generation is being balanced out by antioxidant stimulation. A more likely explanation is that the protocol used was not properly optimized for this specific cell line. Given the issue, the results should be treated as preliminary until repeat testing can be undertaken.

Conclusions and Future Directions

Formaldehyde, cinnamaldehyde, and diacetyl all showed significant effects on various aspects of cellular health. Formaldehyde and cinnamaldehyde seemed to act primarily through cytotoxic and cell death pathways. The main difference between the two was that formaldehyde seemed to have a greater effect on the wild type cells, and cinnamaldehyde seemed to have a greater effect on the knockout cells. Both compounds caused a saturation or overload of the GSH antioxidant system as evidenced by decreased *Gclm* promotor activity and decreased total GSH levels. This raises the issue that, even in individuals with adequate GSH levels or synthesis, subsequent toxic insults could be exacerbated. Diacetyl appeared to act through more cytostatic mechanisms rather than cytotoxic ones. There was actually an increase in the capacity of the GSH antioxidant system, but there were decreases in growth and energy metabolism pathways. This could also potentiate other toxic insults by slowing cell turnover and replacement.

In summary, the data show that there are distinct differences in the effects of formaldehyde, cinnamaldehyde, and diacetyl depending on antioxidant (in this case GSH) status. This could serve well to help focus the scope of future research in an *in vivo* setting using the *Gclm* wild type and null mice previously described. Additionally, a much more in-depth look at the gene expression data and pathway analyses would greatly help with parsing out some of the mechanisms of action of the tested flavoring agents. Looking at the other side of our research question, this study could be repeated in *Gclm* wild type and knockout lung cells to identify differences in potential lung impacts.

References:

[1]Clapp PW & Jaspers I. Electronic Cigarettes: Their Constituents and Potential Links to Asthma. *Current Allergy and Asthma Reports.* 2017; 17(11): 79

[2]Creamer MR, Wang TW, Babb S, et al. Tobacco Product Use and Cessation Indicators Among Adults — United States, 2018. *Morbidity and Mortality Weekly Report*. 2019; 68:1013–1019.

[3]Cullen KA, Ambrose BK, Gentzke AS, Apelberg BJ, Jamal A, & King BA. Notes from the field: Use of Electronic Cigarettes and Any Tobacco Product Among Middle And High School Students—United States, 2011-2018. *Morbidity and Mortality Weekly Report.* 2018; 67(45): 1276-1277.

[4]Cullen KA, et. Al. e-Cigarette Use Among Youth in the United States, 2019. *Journal of the American Medical Association*. 2019; 322(21): 2095-2103

[5]Tsai J, et al. Reasons for Electronic Cigarette Use Among Middle and High School Students—National Youth Tobacco Survey, United States, 2016. *Morbidity and Mortality Weekly Report.* 2018; 67(6): 196-200

[6]Centers for Disease Control and Prevention. Outbreak of Lung Injury Associated with the Use of E-Cigarette, or Vaping, Products. Office on Smoking and Health, National Center for Chronic Disease Prevention and Health Promotion

[7]Rubenstein DA, Hom S, Ghebrehiwet B, & Yin W. Tobacco and e-cigarette products initiate Kupffer cell inflammatory responses. *Molecular Immunology*. 2015; 67(2): 652-660.

[8] Anderson C, Majeste A, Hanus J, & Wang S. E-Cigarette Aerosol Exposure Indices Reactive Oxygen Species, DNA Damage, and Cell Death in Vascular Endothelial Cells. *Toxicological Sciences*. 2016; 154(4): 332-340

[9]Larcombe AN, Janka MA, Mullins BJ, Berry LJ, Bredin A, & Franklin PJ. The Effects of electronic cigarette aerosol exposure on inflammation and lung function in mice. *American Journal of Physiology-Lung Cellular and Molecular Physiology*. 2017; 313: L67-L79

[10] Patro R, Duggal G, & Kingsford C. Salmon: Accurate, Versatile and Ultrafast Quantification from Rna-Seq Data Using Lightweight-Alignment. *BioRxiv*. Cold Spring Harbor Labs Journals 2015, 021592

[11] Soneson C, Love MI, & Robinson MD. 2015. Differential Analyses for Rna-Seq: Transcript-Level Estimates Improve Gene-Level Inferences. *F1000Research.* 2015; 4(1521)

[12] Robinson MD, McCarthy DJ, & Smyth GK. EdgeR: A Bioconductor Package for Differential Expression Analysis of Digital Gene Expression Data. *Bioinformatics.* 2010; 26: 139–40.

[13] Lun ATL, Chen Y, & Smyth GK. 2016. It's de-Licious: A Recipe for Differential Expression Analyses of Rna-Seq Experiments Using Quasi-Likelihood Methods in EdgeR. *Methods in Molecular Biology.* 2016; 391.

[14] Draghici S, et al. A systems biology approach for pathway level analysis. *Genome Research*. 2007; 17(10): 1537-45

[15] Khatri P, Draghici S, Tarca AD, Hassan SS, & Romero R. A system biology approach for the steady-state analysis of gene signaling networks. *Lecture Notes in Computer Science (LNCS)*. 2007; 4756: 32-41

[16] Tarca AL, et al. A novel Signaling Pathway Impact Analysis (SPIA*). Bioinformatics*. 2009; 25(1): 75-82

[17]Klager S, Vallarino J, MacNaughton P, Christiani DC, Lu Q, & Allen JG. Flavoring Chemicals and Aldehydes in E-Cigarette Emissions. *Environmental Science and Technology.* 2017; 51(18): 10806-10813

[18]Chen W, et al. Measurement of heating coil temperature for e-cigarettes with a “top-coil” clearomizer. *PloS One.* 2018; 13(4): e0195925

[19]Ogunwale MA, et al. Aldehyde Detection in Electronic Cigarette Aerosols. *ACS Omega.* 2017; 2(3): 1207-1214

[20]Hjelle JJ & Klaassen CD. Glucuronidation and Biliary Excretion of Acetaminophen in Rats. *Journal of Pharmacology and Experimental Therapeutics.* 1983; 228(2): 407-413

[21]Mitchell JR, Jollow DJ, Potter WZ, Gillette JR, & Brodie BB. Acetaminophen-Induced Hepatic Necrosis. IV. Protective Role of Glutathione. *Journal of Pharmacology and Experimental Therapeutics.* 1973; 187(1): 21-217

[22]McConnachie LA, et al. Glutamate Cysteine Ligase Modifier Subunit Deficiency and Gender as Determinants of Acetaminophen-Induced Hepatotoxicity in Mice. *Toxicological Sciences.* 2007; 99(2): 628-636

[23]Lim J, Nakamura BN, Mohar I, Kavanagh TJ, & Luderer U. Glutamate Cysteine Ligase Modifier Subunit (Gclm) Null Mice Have Increased Ovarian Oxidative Stress and Accelerated Age-Related Ovarian Failure. *Endocrinology.* 2015; 156(9): 3329-3343

[24]Nakamura BN, et al. Increased Sensitivity to Testicular Toxicity of Transplacental Benzo[a]pyrene Exposure in Male Glutamate Cysteine Ligase Modifier Subunit Knockout (Gclm−/−) Mice. *Toxicological Sciences.* 2012; 126(1): 227-241

[25]Hasan KM, et al. E-Cigarettes and Western Diet: Important Metabolic Risk Factors for Hepatic Disease. *Hepatology.* 2019; 69(6): 2442-2454

[26]Behar RZ, et al. Distribution, quantification and toxicity of cinnamaldehyde in electronic cigarette refill fluids and aerosols. *Tobacco Control.* 2016; 25(2): 94-102

[27]Clapp PW, et al. Flavored e-cigarette liquids and cinnamaldehyde impair respiratory innate immune cell function. *American Journal of Physiology Lung Cellular and Molecular Biology.* 2017; 313(2): 278-292

[28]Swales NJ & Caldwell J. Studies on Trans -Cinnamaldehyde II: Mechanisms of Cytotoxicity in Rat Isolated Hepatocytes. *Toxicology in Vitro.* 1992; 10: 37-42

[29]Behar RZ, Luo W, McWhirter KJ, Pankow JF, & Talbot P. Analytical and toxicological evaluation of flavor chemicals in electronic cigarette refill fluids. *Scientific Reports.* 2018; 8(1): 8288

[30]Laskar AA & Younus H. Aldehyde toxicity and metabolism: the role of aldehyde dehydrogenases in detoxification, drug resistance and carcinogenesis. *Drug Metabolism Reviews*. 2019; 51(1): 42-64

[31]Kreiss K, Gomaa A, Kullman G, Fedan K, Simoes EJ, & Enright PL. Clinical Bronchiolitis Obliterans in Workers at a Microwave-Popcorn Plant. *The New England Journal of Medicine.* 2002; 347: 330-338

[32]Allen JG, et al. Flavoring Chemicals in E-Cigarettes: Diacetyl, 2,3-Pentanedione, and Acetoin in a Sample of 51 Products, Including Fruit-, Candy-, and Cocktail-Flavored E-Cigarettes. *Environmental Health Perspectives*. 2016; 124(6): 733-739

[33] Kosmider L, et al. Carbonyl Compounds in Electronic Cigarette Vapors: Effects of Nicotine Solvent and Battery Output Voltage. *Nicotine & Tobacco Research.* 2014; 16(10): 1319-1326

[34] Chen Y, et al. Early Onset Senescence Occurs When Fibroblasts Lack the Glutamate-Cysteine Ligase Modifier Subunit. *Free Radical Biology & Medicine.* 2009; 47(4): 410-418

[35] Paumgartten FJR, Gomes-Carneiro MR, & Oliveira ACAX. The impact of tobacco additives on cigarette smoke toxicity: a critical appraisal of tobacco industry studies. *Cadernos de Saúde Pública.* 2017; 33(3): 39-59

[36] Thielen A, Klus H, & Müller L. Tobacco smoke: unraveling a controversial subject. *Experimental and Toxicologic Pathology.* 2008; 60(2-3): 141-156

[37] Wu D & O'Shea DF. Potential for Release of Pulmonary Toxic Ketene From Vaping Pyrolysis of Vitamin E Acetate. *Proceedings of the National Academy of Sciences of the United States of America.* 2020; 117(12): 6349-6355

[38] Golli NE, et al. Impact of E-Cigarette Refill Liquid With or Without Nicotine on Liver Function in Adult Rats. *Toxicology Mechanisms and Methods.* 2016; 26(6): 419-426

[39]Gloede E, Cichocki JA, Baldino JB, & Morris JB. A Validated Hybrid Computational Fluid Dynamics-Physiologically Based Pharmacokinetic Model for Respiratory Tract Vapor Absorption in the Human and Rat and Its Application to Inhalation Dosimetry of Diacetyl. *Toxicological Sciences.* 2011; 123(1): 231-246

[40]Zhao H, et al. Pharmacokinetic study of cinnamaldehyde in rats by GC–MS after oral and intravenous administration. *Journal of Pharmaceutical and Biomedical Analysis.* 2014; 89: 150-157

[41]Teeguarden JT, Bogdanffy MS, Covington TR, Tan C, & Jarabek AM. A PBPK Model for Evaluating the Impact of Aldehyde Dehydrogenase Polymorphisms on Comparative Rat and Human Nasal Tissue Acetaldehyde Dosimetry. *Inhalation Toxicology.* 2008; 20(4): 375-390

[42]Cederbaum AI. Alcohol Metabolism. *Clinics in Liver Disease.* 2012; 16(4): 667-685

[43]Sasco AJ, Secretan MB, & Straif K. Tobacco smoking and cancer: a brief review of recent epidemiological evidence. *Lung Cancer*. 2004; 45(2): S3-S9

[44]Ambrose JA & Baruna RS. The pathophysiology of cigarette smoking and cardiovascular disease: An update. *Journal of the American College of Cardiology.* 2004; 43(10): 1731-1737

[45]Im H, et al. Evaluation of Toxicological Monitoring Markers Using Proteomic Analysis in Rats Exposed to Formaldehyde. *Journal of Proteome Research.* 2006; 5(6): 1354-1366

[46]Formaldehyde, 2-Butoxyethanol and 1-tert-Butoxypropan-2-ol. *IARC Monographs on the Evaluation of Carcinogenic Risks to Humans.* 2006; 88

[47]Lu SC. Glutathione Synthesis. *Biochimica et Biophysica Acta,* 2013; 1830(5): 3143-3153

[48]Espinoza-Derout J, et al. Hepatic DNA Damage Induced by Electronic Cigarette Exposure Is Associated With the Modulation of NAD+/PARP1/SIRT1 Axis. *Frontiers in Endocrinology (Lausanne).* 2019; 10: 320

[49]Crotty Alexander LE, et al. Chronic inhalation of e-cigarette vapor containing nicotine disrupts airway barrier function and induces systemic inflammation and multiorgan fibrosis in mice. *American Journal of Physiology. Regulatory, Integrative, and Comparative Physiology.* 2018; 314(6): R834-R847

[50]Johansson E, Wesselkamper SC, Shertzer HG, Leikauf GD, Dalton TP, & Chen Y. Glutathione deficient C57BL/6J mice are not sensitized to ozone-induced lung injury. *Biochemical and Biophysical Research Communications.* 2010; 396(2): 407-412

[51]Melnikov F, et al. Kinetics of Glutathione Depletion and Antioxidant Gene Expression as Indicators of Chemical Modes of Action Assessed in Vitro in Mouse Hepatocytes with Enhanced Glutathione Synthesis. *Chemical Research in Toxicology.* 2019; 32: 421-436

Supplemental Protocols and Figures:

Supplemental Protocol 1: Example Viability Assay (alamarBlue)

- Pass and plate cells at a density of 22k cells/well (*Gclm* WT) and 40k cells/well (*Gclm* KO)
    - See plate map below for layout
    - Be sure to pipette up and down between rows to ensure equal mixing
    - After cells plated, pipette up and down in wells to ensure uniform distribution
- Incubate cells for 24 hours at 33℃, 5% CO2
- Prepare stock solutions of reagents
    - For 2 mL 100 mM hydroquinone solution:
        - Add 0.022 g solid hydroquinone to 2 mL H_2O
    - For 3ml 100 mM acetaldehyde solution (due to potential hazard):
        - Add 26 µL concentrated diacetyl to 3 mL H_2O (density = .99 g/mL)
- Prepare working solutions of reagents for a dose series of 1 mM, 750 µM, 500 µM, 250 µM, 100 µM, and 10 µM
    - Diacetyl solutions, using the 100 mM stock:
        - 1 mM: Add 50 µL of 100 mM to 5 mL media
        - 750 µM: Add 1.2 mL of 1 mM to 400 µL media
        - 500 µM: Add 2 mL of 1 mM to 2 mL media
        - 250 µM: Add 1 mL of 500 µM to 1 mL media
        - 100 µM: Add 500 µL of 500 µM to 2 mL media
        - 10 µM: Add 200 µL of 100 µM to 1.8 mL media
- Prepare 100 µM hydroquinone for WT positive control and 50 µM hydroquinone for KO positive control from 100 mM stock
    - For 100 µM solution:
        - Add 3µL 100 mM stock to 3 mL medium
    - For 50 µM solution:
        - Add 1 mL 100 µM solution to 1 mL medium
- Filter sterilize all working solutions before dosing cells
- Dose cells as described on plate map
- Incubate for 24 hours at 33 ℃, 5% CO2
- Run alamarBlue viability assay
    - Add 10 µL of 10x premade alamarBlue solution to each well
    - Make sure to have appropriate controls—media plus alamar with no cells, and media alone
    - Incubate at 33 ℃ for 2 hours protected from light
    - Read fluorescence using an excitation wavelength of 560 nm (540-570 nm range) and an emission wavelength of 590 nm (580-610 nm range)
- Fix cells
    - Dropwise, add 4% paraformaldehyde solution to each well with cells
    - Let plate sit at room temperature for 60 minutes

- Wash cells with 200 µL PBS
- Prepare and run Hoechst-42 assay to establish the number of intact cells in each well
    - Dilute the 1mg/ml stock Hoechst solution to a concentration of 2 µg/mL
        - Add 20 µL of 1 mg/mL stock to 10 mL PBS
    - Add 100 µL solution to each well with cells, and some non-celled wells to run as a control
    - Incubate at room temp or 37 ℃ for 15 minutes in the dark
- Take plate reading at excitation and emission wavelengths of 350 nm and 460 nm

Supplemental Protocol 2: GCLM Promotor Activity (DDAOG Assay)

- Only use *Gclm* KO cells for this assay, as *Gclm* WT cells do not have the knock-in β-Gal gene
- Cells should already be fixed and in 100 µL of 2 µg/mL Hoechst/PBS solution
- Each plate should have 3-4 replicates of all doses used in viability assays, including negative controls (complete media only) and positive controls (50 µM hydroquinone)
- Remove Hoechst solution from KO cells
- Wash with 200 µL PBS and allow to sit for 5 minutes
    - While waiting, make DDAOG working solution by adding 10 µL of DDAOG stock per 1 mL PBS
    - Make sure work is done in the dark due to DDAOG's fluorescent properties
- Remove PBS wash and add 200 µL of DDAOG working solution
- Wrap plate in foil and incubate at 4 ℃ for up to 24 hours
    - Longer incubation times give greater separation between blanks and samples
- Allow plate to warm to room temperature before reading fluorescence
- Measure fluorescence using an excitation emission profile of 633 nm/670 nm
    - Use endpoint setting with top read

Supplemental Protocol 3: Total Glutathione Quantitation (NDA Assay)

Adapted from the Protocols of White CC and Botta D

<u>Reagents used:</u>

- TES/SB buffer—leftmost refrigerator, top shelf
- Protease inhibitor (100x)—leftmost refrigerator, second shelf from top
- 10% and 5% SSA (sulfosalicylic acid)—leftmost refrigerator, top shelf
- 0.5 N NaOH
- 0.2 M NEM (n-ethylmorpholine)/0.02 M KOH
- GSH—leftmost refrigerator, desiccator
- TCEP—leftmost refrigerator, desiccator
- NDA—leftmost refrigerator, desiccator

To do the day prior

1. Label microfuge tubes in advance
    a. Label 1.7 mL tubes with brief identifier of tube contents (these will not be the final storage tubes)
    b. Label 1.5 mL or 1.7 mL tubes with more comprehensive identifiers including: compound, dose, cell line, replicate number, date, and the word "Centrifuged"

Harvesting cells:

1. After 24-hour dosing period is complete, remove dosed media from each well and rinse with PBS
    a. There should be three wells for each dose: completed media only (negative control), 100 µM/50 µM hydroquinone (WT and KO positive control), and three doses of each specific compound
2. Add 350 µL TES/SB+1x protease inhibitor (dilute 1:100) to each well
3. Using a cell scraper, scrape the cells attached to the bottom of each well into the liquid
    a. With a P-1000 pipettor, rinse the wells just above the liquid line to ensure maximal recovery of cells
    b. Use a separate scraper for each cell type and compound
4. Transfer cell solution to labelled 1.7 mL microfuge tubes and place on ice

Initial (Day 1) sample prep:

1. Sonicate all tubes at 40 mA using two 5 second pulses and a 5 second break in-between
    a. Make sure to wipe the sonicator rod down with alcohol between tubes
    b. Return sonicated tubes to ice bucket
2. Transfer ~150 µL of lysate to another set of labelled 1.7ml microfuge tubes containing an equal volume of 10% SSA—this will be used for GSH quantitation
3. Centrifuge the non-SSA lysate at 15k x g for 20 minutes in the walk-in cooler
4. Centrifuge the SSA lysate at 13k x g for 2 minutes in the walk-in cooler
5. Transfer the supernatants from each tube into clean 1.5 mL or 1.7 mL tubes
    a. Be sure not to touch or transfer any of the resulting pellet material
6. Samples can be stored at -80 ˚C until rest of assay is to be run

Final (Day 2) sample prep:

1. If samples were stored at -80 ˚C, thaw tubes in ice
2. Bring dry reagents (GSH, TCEP, and NDA) to room temp
3. While everything is warming, test the pH for each step in empty tubes
    a. Add 25 µL (sample volume) of 5% SSA to each tube
    b. To one of those tubes, add 80 µL NEM/KOH and ensure the pH is 7-8
    c. Adjust NEM/KOH volume and continue testing pH in new tubes until appropriate pH is reached
    d. To a tube with the appropriate amount of SSA and NEM/KOH, add 50 µL NaOH
    e. The pH of this solution should be ~12.5; anything over 13 will ruin reaction

4. Weigh out 30.7 mg GSH and add to 10 mL 5% SSA
5. Prepare GSH standard curve, being sure to keep everything on ice (only use *italicized* concentrations):

Concentration	**GSH Standard Soln**	**5% SSA**
10 mM	30.7 mg stock powder	10 mL
1 mM	100 µL of 10 mM	900µL
0.5 mM	*50 µL of 10 mM*	*950µL*
0.25 mM	*25 µL of 10 mM*	*975µL*
0.1 mM	*100 µL of 1 mM*	*900µL*
0.075 mM	*75 µL of 1 mM*	*925µL*
0.05 mM	*50 µL of 1 mM*	*950µL*
0.025 mM	*25 µL of 1 mM*	*975µL*
0.01 mM	*10 µL of 1 mM*	*990µL*
0 mM	*NONE*	*1000µL*

6. Weigh out 3.7 mg NDA and transfer to a 1.7 mL tube on ice
    a. Add 2 mL DMSO right before using, and mix by inverting—DO NOT VORTEX
7. Weigh out 2.86 mg (or a multiple) TCEP and transfer to a 1.7 mL tube on ice
    a. Add 1 mL (or a multiple) DI H_2O right before use and mix well

Setting up the plate:

1. Add 25 µL of standard or sample to the wells of a black, flat-bottom microplate in triplicate
2. Add 80 µL NEM/KOH buffer to each well using a multichannel pipette
3. Add 10 µL TCEP to each well using a repeater pipette and vortex plate to mix
    a. Let stand for 15 minutes at RT
4. Add 50 µL NaOH using a multichannel pipette
5. Add 10 µL NDA with a repeater pipette and vortex plate to mix
    a. Let stand for 30 minutes at RT in the dark (in foil)

Plate reader settings:

1. Read plate using an excitation/emission profile of 472 nm/528 nm
2. Plate reader should be taking a top endpoint reading with 20 flashes per read

Supplemental Protocol 4: Lipid Peroxidation (TBARS Assay)

- Plate cells to ensure 70% confluency by the time of dosing in a 6-well plate
    - *Gclm* WT: 330k/well (1 day settle); 190k/well (2 day settle)
    - *Gclm* KO: 700k/well (1 day settle); 500k/well (2 day settle)
- Dose cells using the following doses (should allow for decent effects while leaving enough cells for assay):
    - PFA: 50 µM and 200 µM
    - Acetaldehyde: 1 µM and 1 mM

    - Cinnamaldehyde: 10 µM and 100/50 µM (WT/KO)
    - Diacetyl: 250 µM and 1 mM
    - Hydroquinone: 100 µM (WT) and 50 µM (KO)
        - These will serve as positive controls
    - One well should only have completed media only to act as a negative control
- After dosing period, remove media and wash cells gently with PBS
- Aspirate PBS and add 300 µL of MDA Lysis Buffer with 3 µL of 100x BHT added
    - Total volume per run: 6 mL buffer + 60 µL BHT
- Scrape cells off plate and transfer lysis solution to a 1.7 mL tube on ice
- Sonicate samples on ice to homogenize
- Centrifuge samples at 13000 x g for 10 minutes
- While samples are spinning, make MDA standards
    - 0.1 M: 10 µL of 4.17 M MDA stock + 407 µL DI H_2O
    - 2 mM: 20 µL of 0.1 M solution + 980 µL DI H_2O
    - 0.2 mM: 100 µL of 2 mM solution + 900 µL DI H_2O
    - 2 nmol (10 µM): 10 µL of 0.2 mM + 190 µL DI H_2O
    - 1.6 nmol (8 µM): 8 µL of 0.2 mM + 192 µL DI H_2O
    - 1.2 nmol (6 µM): 6 µL of 0.2 mM + 194 µL DI H_2O
    - 0.8 nmol (4 µM): 4 µL of 0.2 mM + 196 µL DI H_2O
    - 0.4 nmol (2 µM): 2 µL of 0.2 mM + 198 µL DI H_2O
    - 0 nmol (0 µM): 200 µL DI H_2O
- Transfer 200 µL of supernatant from centrifuged tubes to a new 1.7 mL tube
    - Run protein assay on insoluble fraction left behind after centrifugation
- Make working TBA solution
    - To the powdered stock, add 7.5 mL glacial acetic acid
    - Gently shake bottle to mix, and transfer contents to a 50 mL tube
    - Adjust the final volume to 25 mL using DI H_2O
- Add 600 µL of TBA solution to each vial of sample and standard
- Incubate samples and standards at 95 ℃ for 60 minutes
- Cool samples to room temperature in an ice bath for 10 minutes
- Pipette 200 µL from each mixture into a 96-well plate in triplicate
- Measure fluorescence using an excitation/emission of 532 nm/553 nm

Supplemental Protocol 5: Protein Quantitation

Assay prep:

1. Thaw out protein tubes for respective NDA assay on ice
2. Thaw out BSA standards located in the leftmost freezer in the marked bag
    a. Standards include: 0 mg/mL, 0.05 mg/mL, 0.1 mg/mL, 0.15 mg/mL, 0.2 mg/mL, 0.25 mg/mL, 0.3 mg/mL, and 0.35 mg/mL
3. Set up plate reader to report an A_{595} using a top endpoint reading at 20 flashes per read

4. Prepare working dye solution by adding 1 part stock dye (located in middle 4 ˚C refrigerator) to 4 parts DI H_2O
5. Dilute samples 1:2 or 1:3 to ensure linear range

Running the assay:

1. Add 10 µL of diluted sample or BSA standard in triplicate
2. Add 200 µL working dye solution to each well
3. Vortex plate to mix well
4. Can read plate immediately after mixing

Troubleshooting:

1. Retest samples with higher dilutions if still outside linear range of standard curve
    a. Note retested samples to ensure clarity

Supplemental Figure 1

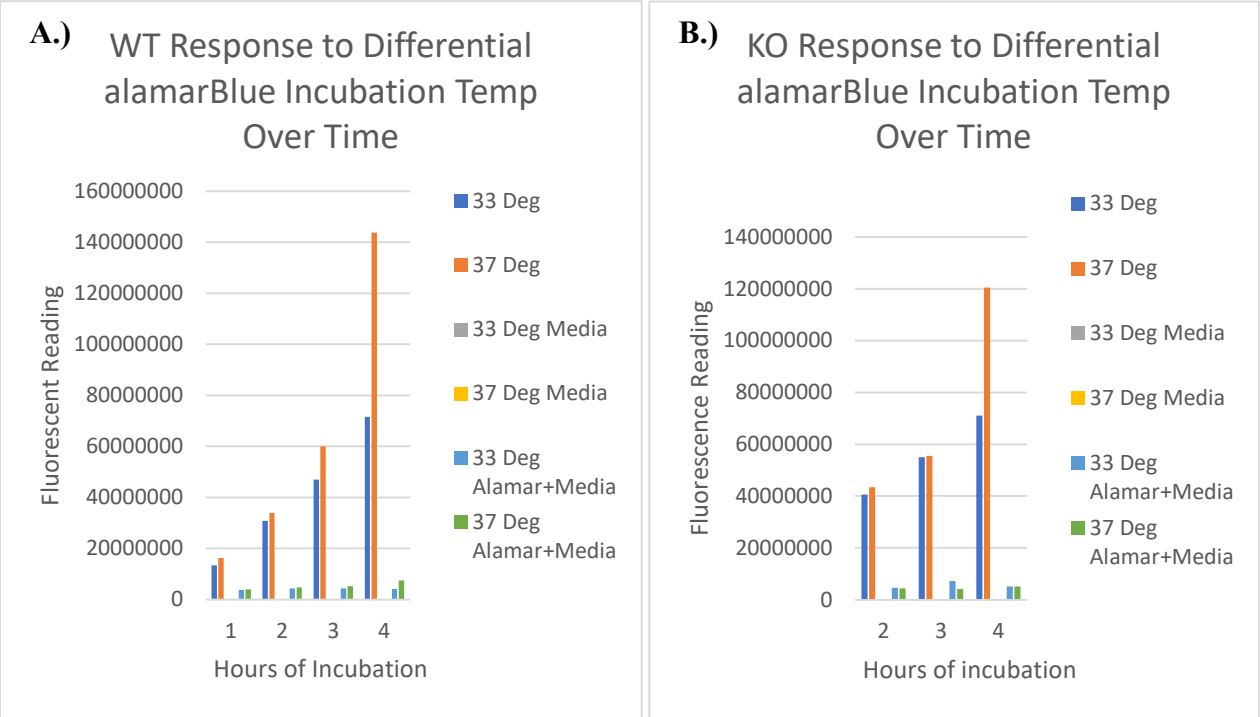

Rationale for adjusting manufacturer's suggested protocol for the alamarBlue assay. Graphs represent the comparative responses in alamarBlue fluorescence at multiple incubation temperatures and time periods for **A.)** wild type cells and **B.)** knockout cells. Due to both cell lines' sensitivity to 37℃ incubation, 33℃ was preferred. In both cell lines, both 37℃ and 33℃ readings were similar up until two hours of incubation. Longer incubation times showed increasing variability between temperatures. Thus, a two-hour incubation time was chosen at 33℃.

Supplemental Figure 2

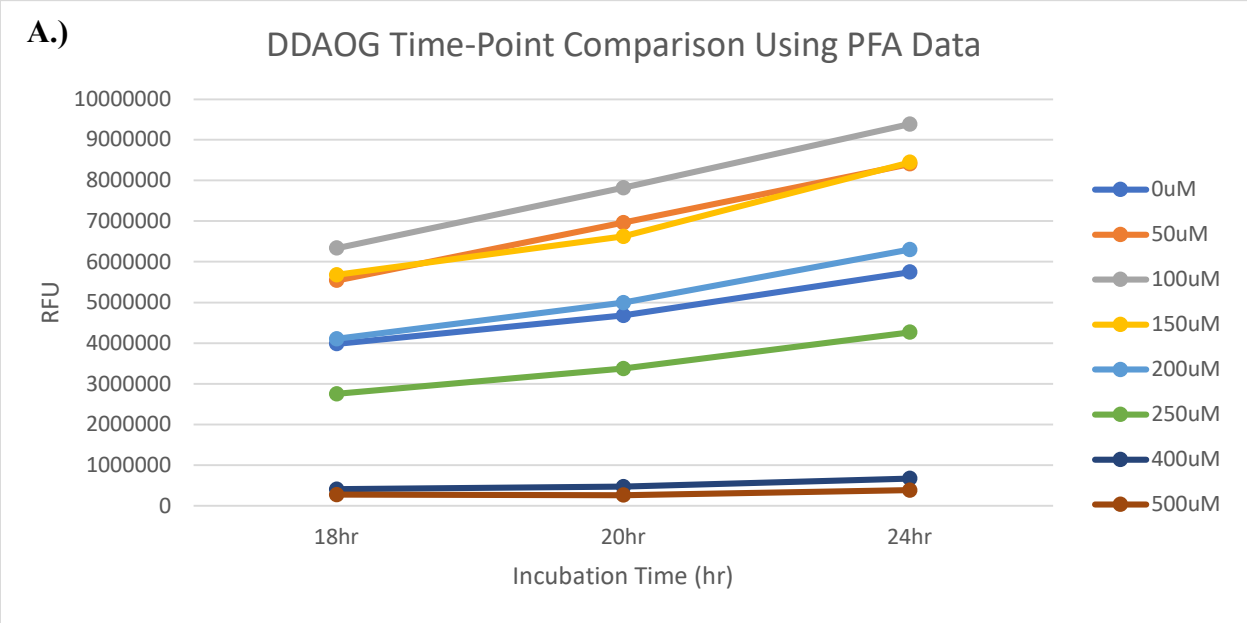

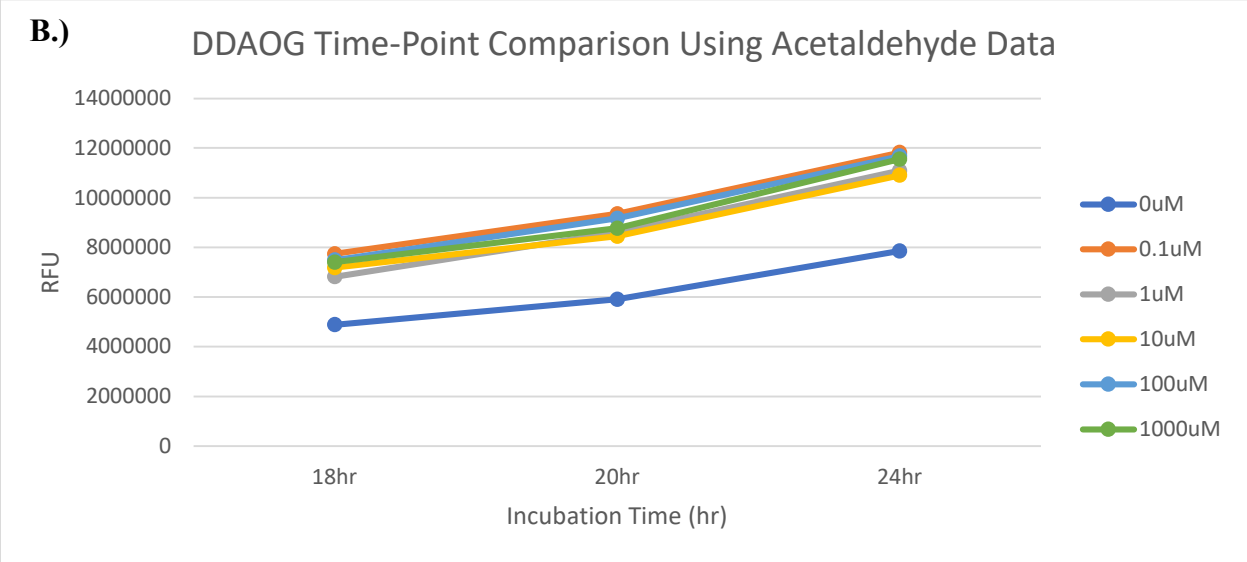

Rationale for the chosen incubation time for DDAOG assays. The original protocol suggested incubating plates at 4°C overnight. The goal was to find a specific time-point that allowed for a good separation of sample fluorescence from background fluorescence while not having a scenario where all the DDAOG substrate has been converted to fluorescent product. Therefore, a more specific incubation time frame of 20-24 hours was chosen based on the trends shown.

Supplemental Figure 3

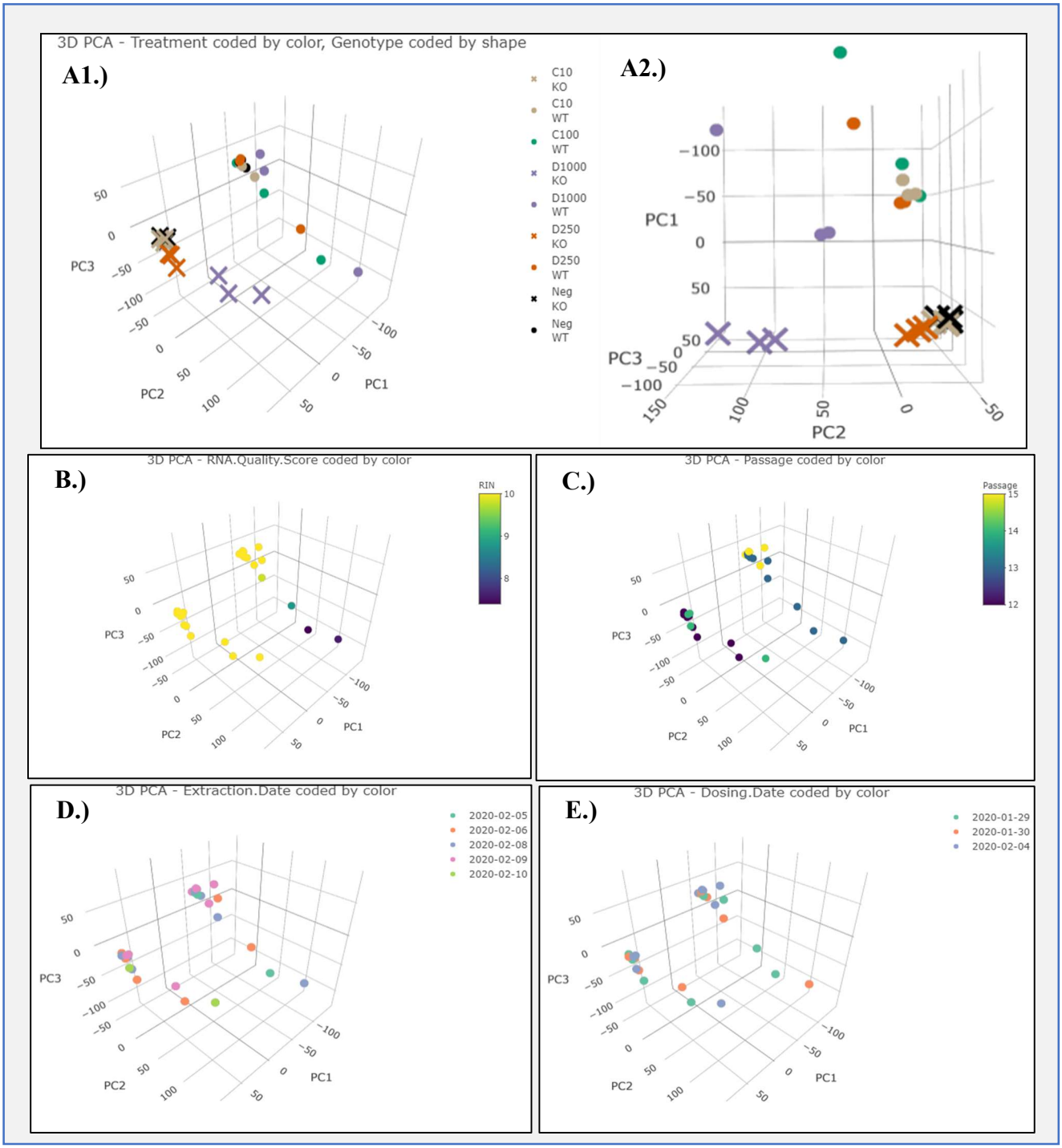

PCA plots coded by dose/genotype (**A1** and **A2**), RNA quality (**B**), cell passage number (**C**), RNA extraction date (**D**), and dosing date (**E**). **A1** and **A2** are two different views of the same plot

Supplemental Figure 4

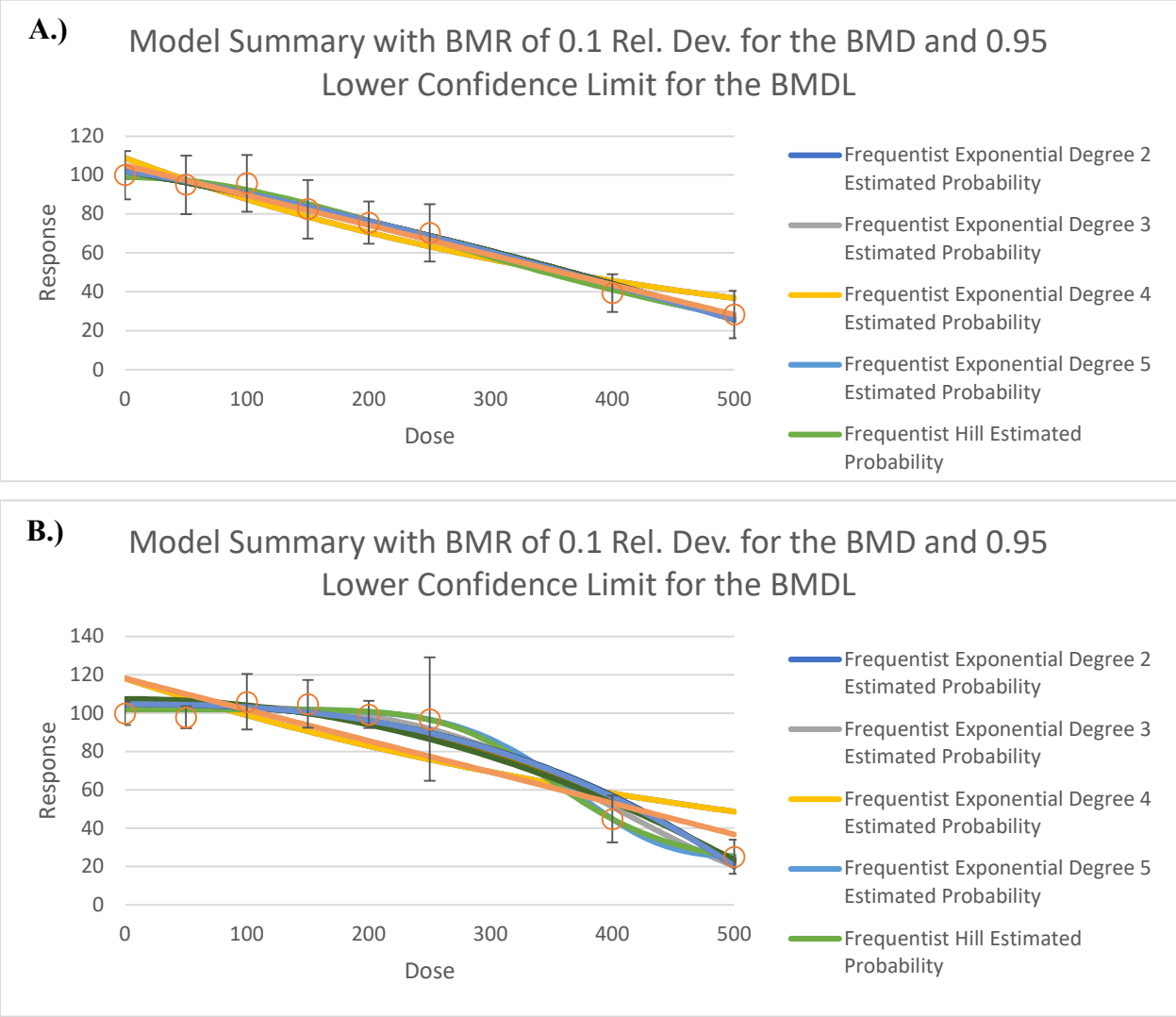

Graphical outputs of the EPA's BMD modeling software for **A.)** wild type and **B.)** knockout cells when exposed to formaldehyde. Individual data points represent the average viability as a percent of negative control across all experiments run for formaldehyde. Each colored line represents a different model.

Supplemental Figure 5

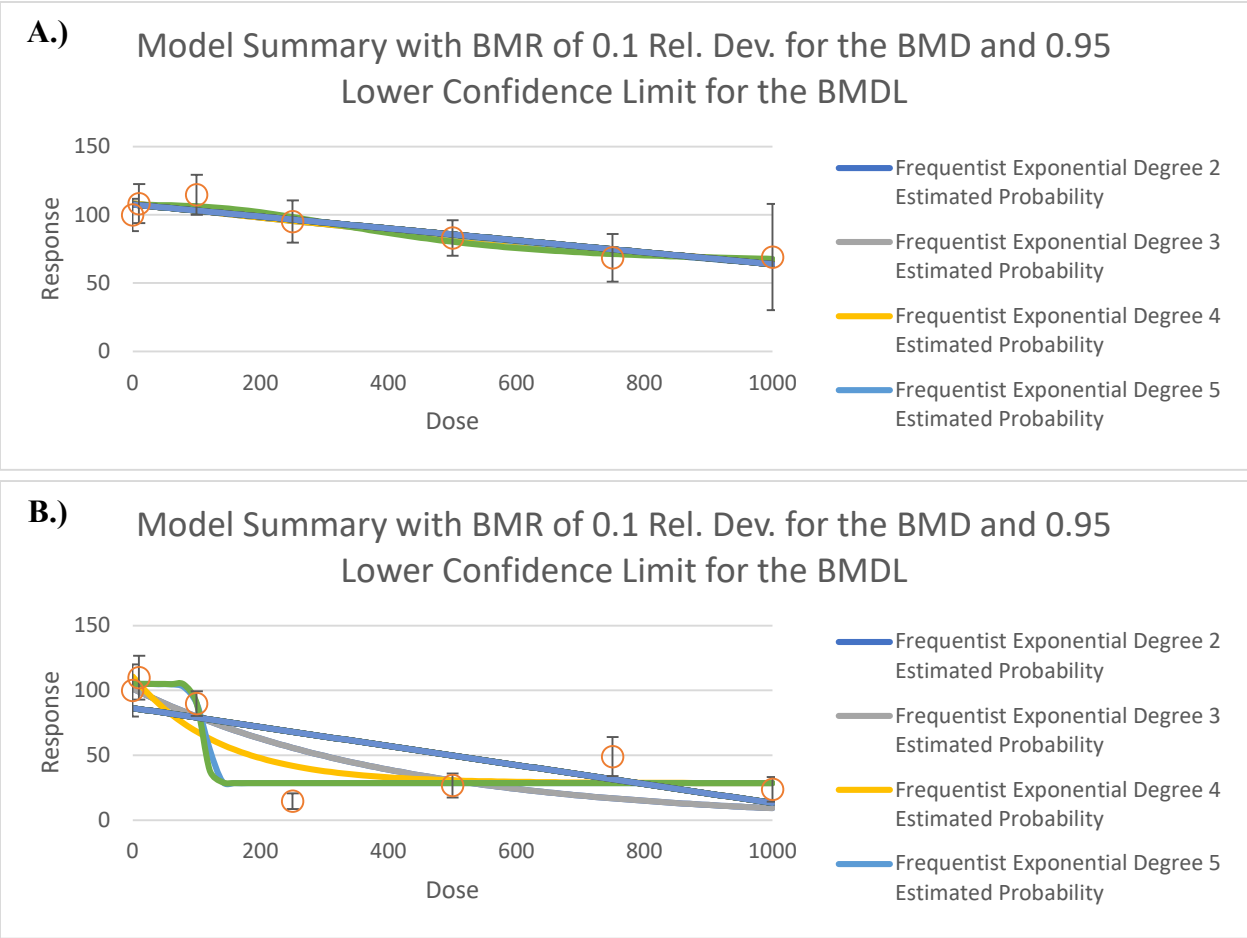

Graphical outputs of the EPA's BMD modeling software for **A.)** wild type and **B.)** knockout cells when exposed to cinnamaldehyde. Individual data points represent the average viability as a percent of negative control across all experiments run for cinnamaldehyde. Each colored line represents a different model.

Supplemental Figure 6

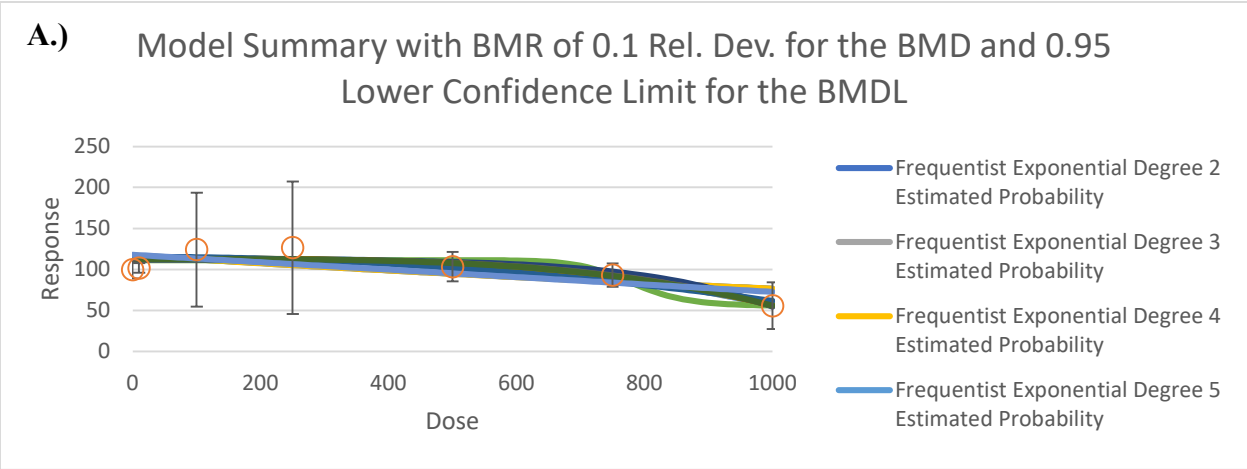

Graphical outputs of the EPA's BMD modeling software for wild type cells when exposed to diacetyl. Individual data points represent the average viability as a percent of negative control across all experiments run for diacetyl. Each colored line represents a different model.

Supplemental Figure 7

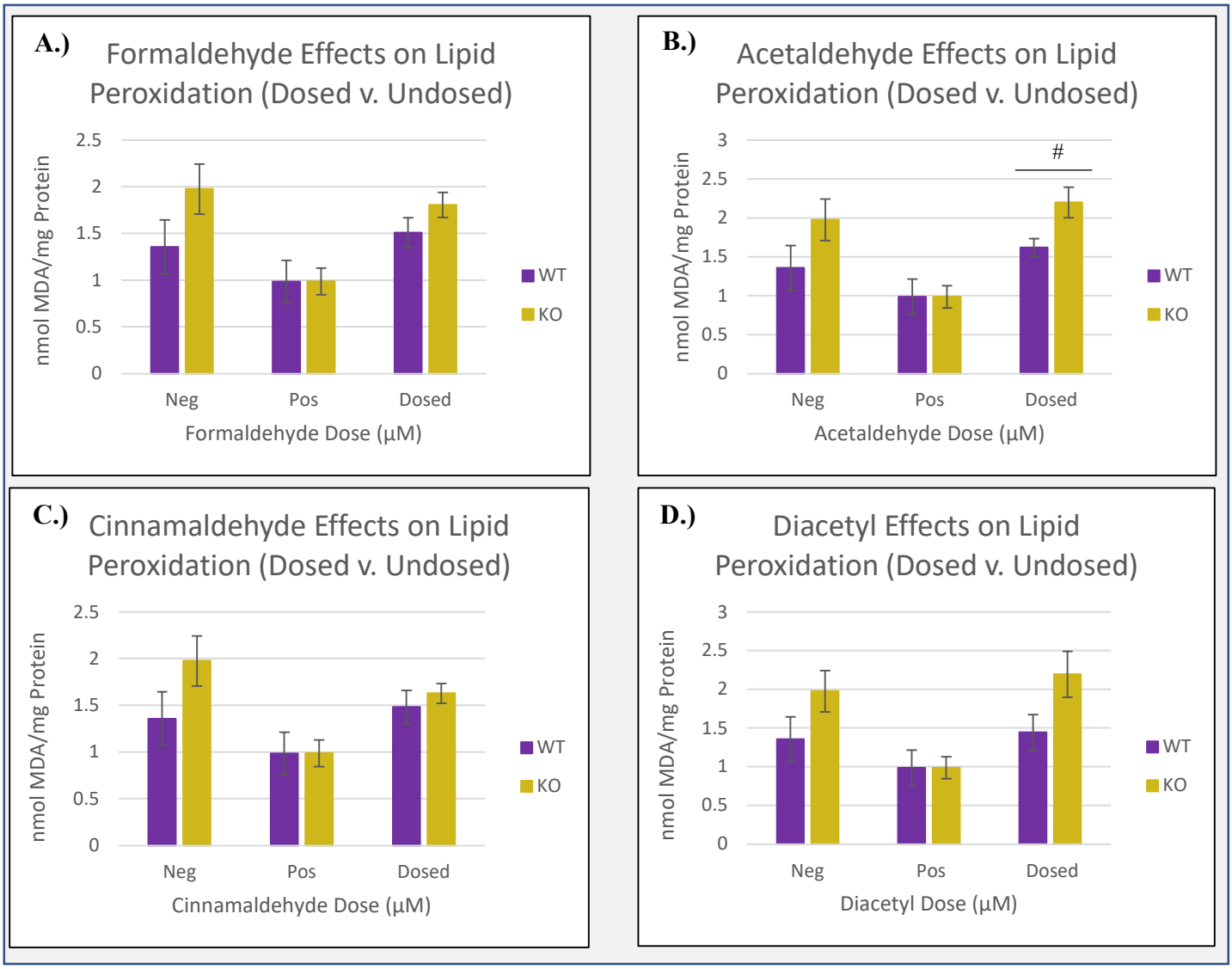

Graphical representations of lipid peroxidation levels when *Gclm* wild type and knockout cells were exposed to (**A**) formaldehyde, (**B**) acetaldehyde, (**C**) cinnamaldehyde, and (**D**) diacetyl. Plots were generated by aggregating protein standardized lipid peroxidation levels of all doses for each compound. Data is displayed as the average +/- SEM.
Genotype significance: # = $0.01 \leq P < 0.05$; ## = $0.001 \leq P < .01$; ### = $P < 0.001$